TIC

COO-1591-29
UTEC MSE 75-188
December 1975

IMPURITY EFFECTS ON THE CREEP OF POLYCRYSTALLINE MAGNESIUM AND ALUMINUM OXIDES AT ELEVATED TEMPERATURES

Ronald S. Gordon
Principal Investigator

Copy of ERDA Form 427 is attached. 1/19/76

Technical Progress Report
December 19, 1974 to December 18, 1975

Energy Research and Development Administration

Contract No. E(11-1)-1591

Department of Materials Science and Engineering

University of Utah

Salt Lake City, Utah 84112

DISCLAIMER

TECHNICAL PROGRESS REPORT

December 18, 1975

PROJECT TITLE	Impurity Effects on the Creep of Polycrystalline Magnesium and Aluminum Oxides at Elevated Temperatures
CONTRACT	E(11-1)-1591
CONTRACTOR	University of Utah Department of Materials Science & Engineering
PERIOD REPORTED	December 19, 1974 to December 18, 1975
PROJECT PERSONNEL	Principal Investigator

Dr. Ronald S. Gordon
Professor

Graduate Research Assistants

Mr. Paul A. Lessing

Mr. Yasuro Ikuma

Undergraduate Assistant

Mr. James D. Hodge

Mr. Robin Chopyk

TABLE OF CONTENTS

ABSTRACT

The research described in this report and the attached reprints covers work on:

1. Viscous creep of fine-grained MgO doped with iron
2. The effects of transition metal impurities and grain size on the creep of polycrystalline Al_2O_3
3. The non-viscous creep of large grain size MgO and Al_2O_3, pure and doped with transition metal impurities
4. Stress relaxation tests on polycrystalline MgO and Al_2O_3, pure and doped with transition metal impurities
5. The construction of creep deformation maps for polycrystalline MgO and Al_2O_3, pure and doped with iron
6. Preliminary studies on the effect of grain size on the creep of polycrystalline mullite

Some of the significant findings include:

1. Power law creep ($N \sim 3$) in polycrystalline MgO is independent of iron doping, grain size, and oxygen partial pressure
2. Three will defined regimes have been identified for the diffusional creep of polycrystalline MgO and Al_2O_3, pure and doped with transition metal impurities: (1) cation grain boundary diffusion (2) cation lattice diffusion, (3) anion grain boundary diffusion
3. Coble diffusional creep, which is rate-limited by oxygen grain boundary diffusion, has been identified in reduced iron-doped (2 cation %) and double doped (1/4% Mn and 1/4% Ti) polycrystalline Al_2O_3
4. Stress relaxation deformation tests can be used to (1) identify transitions between viscous and non-viscous deformation, and (2) achieve high stresses ($\sim 10^3$ kg/cm^2) and strain rates ($1h^{-1}$) without fracture. Good agreement exists between dead-load creep and stress relaxation studies in four point bending.

I. INTRODUCTION

The research activities under contract E(11-1)-1591 during the period December 19, 1974 to December 18, 1975 are described in this report and in the attached reprint (1).

Major effort was devoted to the following:

1. Additional data on grain size effects on the creep of polycrystalline MgO have been obtained at two dopant levels (0.05 and 5.3 cation % Fe). These data in combination with previous measurements made during the course of the contract were used to study the effect of iron dopant concentration on the important mass transport parameters in polycrystalline MgO.

2. The effect of grain size on the creep of pure and doped polycrystalline Al_2O_3 was determined in the low stress regime at 1450°C. Dopants studied were (in cation %) 0.2, 1 and 2% Fe, 1 and 10% Cr, and 1/4% Mn - 1/4% Ti (and 1/4% Ti - 1/4% Cu). Excellent examples of Coble creep were encountered in two situations: (1) 2% Fe under reducing conditions ($P_{O_2} \sim 10^{-7}$ atm). (2) Double dopant of 1/4% Mn and 1/4% of Ti.

3. Dead-load creep experiments were conducted on coarse-grained (40-1200μm) polycrystalline Al_2O_3, pure and doped with chromium (1 and 10%). For undoped Al_2O_3 creep rates increased with increasing grain size while in the case of chromium-doped material creep rates were independent of grain size.

4. Stress relaxation deformation studies in bending were continued in polycrystalline MgO and Al_2O_3, pure and doped with transition metal impurities (Fe,Cr). Tests which reached high stresses ($\sim$ 1000 kg/cm^2) and strain rates (1 h^{-1}) without fracture helped to delineate transitions between viscous and non-viscous creep. Excellent correlation existed between stress relaxation and dead-load creep measurements providing center point deflections were measured in the relaxation experiments.

5. Using the data which have been accumulated over the course of this contract, several creep deformation maps were constructed for polycrystalline MgO and Al_2O_3, pure and doped with iron. These maps illustrate the important deformation mechanisms which operate in these systems and the range of variables (stress, temperature, and grain size) over which they are dominant.

6. Additional studies were conducted on polycrystalline mullite to investigate the effect of grain size on the steady state creep properties.

Four papers have been published this year. Copies of the available reprints [1,3,4] are attached to this report:

1. "Creep of Polycrystalline Mullite", P. A. Lessing, R. S. Gordon, and K. S. Mazdiyasni, J. Amer. Ceram. Soc. 58 (3-4) 149 (1975).

2. "Impurity and Grain Size Effects on the Creep of Polycrystalline Magnesia and Alumina", Paul A. Lessing and Ronald S. Gordon in Deformation of Ceramic Materials, edited by R. C. Bradt and R. E. Tressler, pp. 271-296, Plenum Press, N. Y., (1975).

3. "Ambipolar Diffusion and its Application to Diffusion Creep", Ronald S. Gordon, in Mass Transport Phenomena in Ceramics, edited by A. R. Cooper and A. H. Heuer, pp. 445-464, Plenum Press, N. Y., (1975).

4. "Analysis of Mass Transport in the Diffusional Creep of Polycrystalline MgO-FeO-Fe_2O_3 Solid Solutions", R. S. Gordon and J. D. Hodge, J. Mater. Sci., 10 200-204, (1975).

A complete listing of the bibliography of papers and theses prepared under this contract is given at the end of the report in Section IV.

Finally, the principal investigator presented an invited lecture at a special meeting of the Japanese Ceramic Society in Tokyo on June 28, 1975. The presentation was entitled, "Impurity and Grain Size Effects on the High Temperature Creep of Polycrystalline Al_2O_3 and MgO".

II. REVIEW OF RESEARCH ACTIVITIES

In this section the research activities which have been conducted under the contract for the current period will be described.

2.1 Viscous Creep of MgO-FeO-Fe_2O_3 Solid Solutions

This year additional data on grain size effects in the creep of polycrystalline MgO have been obtained at two dopant levels (0.05 and 5.3 cation % Fe) in creep tests at 1350°C. These data in combination with previous measurements made during the course of the contract permit some conclusions to be drawn concerning the effects of doping on the important transport parameters in polycrystalline MgO.

2.1.1 Grain Size Effects in Dilute MgO-FeO-Fe_2O_3 Solid Solutions (0.05 cation %)

Using a technique developed by Terwilliger, et al, [5] and applied last year [6] to the creep of "pure" polycrystalline MgO, additional experiments were conducted during the current period at the 0.05 cation % dopant level at 1350°C. In this method, previously obtained grain growth data are used to assign grain sizes to the creep specimen at various times during the deformation test. By plotting the assigned grain sizes against the corresponding creep rates, the grain size dependence can be determined from the decay in strain rate due to the occurrence of simultaneous grain growth.

In Figure 1 grain growth data at 1350°C are shown for polycrystalline MgO doped with 0.05 % Fe. Included in the plot are grain sizes of the specimens after creep testing for various periods of time at 1350°C. These data indicate that grain growth in the control specimens is comparable to that observed in specimens which were creep tested at the same temperature. All grain sizes were determined on polished surfaces using the linear intercept method by counting $\sim$ 500 grains. Grain sizes in Figure 1 are reported as

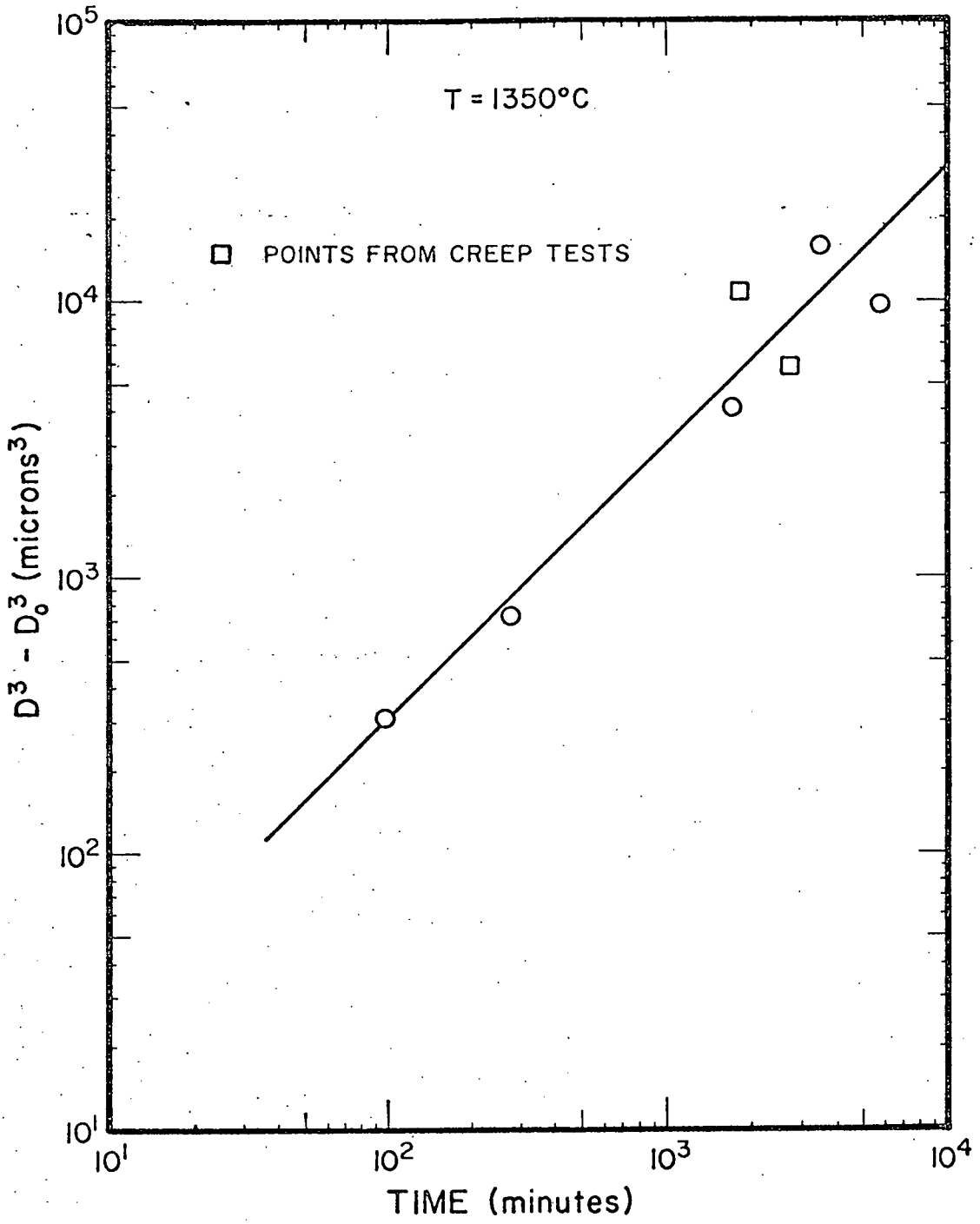

Figure 1 Grain Growth at 1350°C in Polycrystalline MgO Doped with 0.05 cation % Iron

linear intercepts. On all other figures in this report they are reported as the linear intercept value multiplied by 1.5 unless indicated otherwise.

The grain growth data in Figure 1 follow cubic kinetics (i.e. $D^3 - D_o^3 = KT$), a result in good agreement with previously reported data by Gordon, et al. [7] at 1400°C and 1500°C at the same dopant level. The grain growth rates are also consistent with the earlier work. All specimens for the grain growth and creep studies were over 99% dense.

Using the grain growth data in Figure 1 in combination with dead-load creep data at the same temperature, the effect of grain size on the viscous creep of polycrystalline MgO doped with 0.05 cation % Fe was determined at 1350°C in the regime of low stress (<100 kg/cm^2). These results, which are shown in Figure 2, reveal grain size exponents ranging between 2.67 and 2.86 which are indicative of a viscous creep process in which transport by both magnesium grain boundary ($\delta_{Mg}D^b_{Mg}$) and magnesium lattice diffusion (D^ℓ_{Mg}) is comparable. Terwilliger, et al. reported a grain size exponent of ~ 3 in creep tests at 1350°C in material at the same dopant concentration. Values of D^ℓ_{Mg} and $\delta_{Mg}D^b_{Mg}$ equal to $(2.35 - 7.17) \times 10^{-13}$ cm^2/sec and $(6.79 - 7.76) \times 10^{-16}$ cm^3/sec, respectively, were calculated by a procedure described in last year's report [6]. It is noted that $\delta_{Mg}D^b_{Mg}$ is relatively insensitive to changes in the value of m, while D^ℓ_{Mg} is very sensitive to similar changes. Additional experiments will be conducted to stabilize the experimental value of the grain size exponent. The significance of these calculations will be discussed in a subsequent section of this report.

2.1.2 Grain Size Effects in Concentrated MgO-FeO-Fe_2O_3 Solid Solutions (5.3 cation % Fe)

Prior to this year very little data have been available to characterize the creep rate - grain size dependence at the 5.3% dopant level (the upper limit for the iron dopant concentration in studies to date). Tremper, et al. [8]

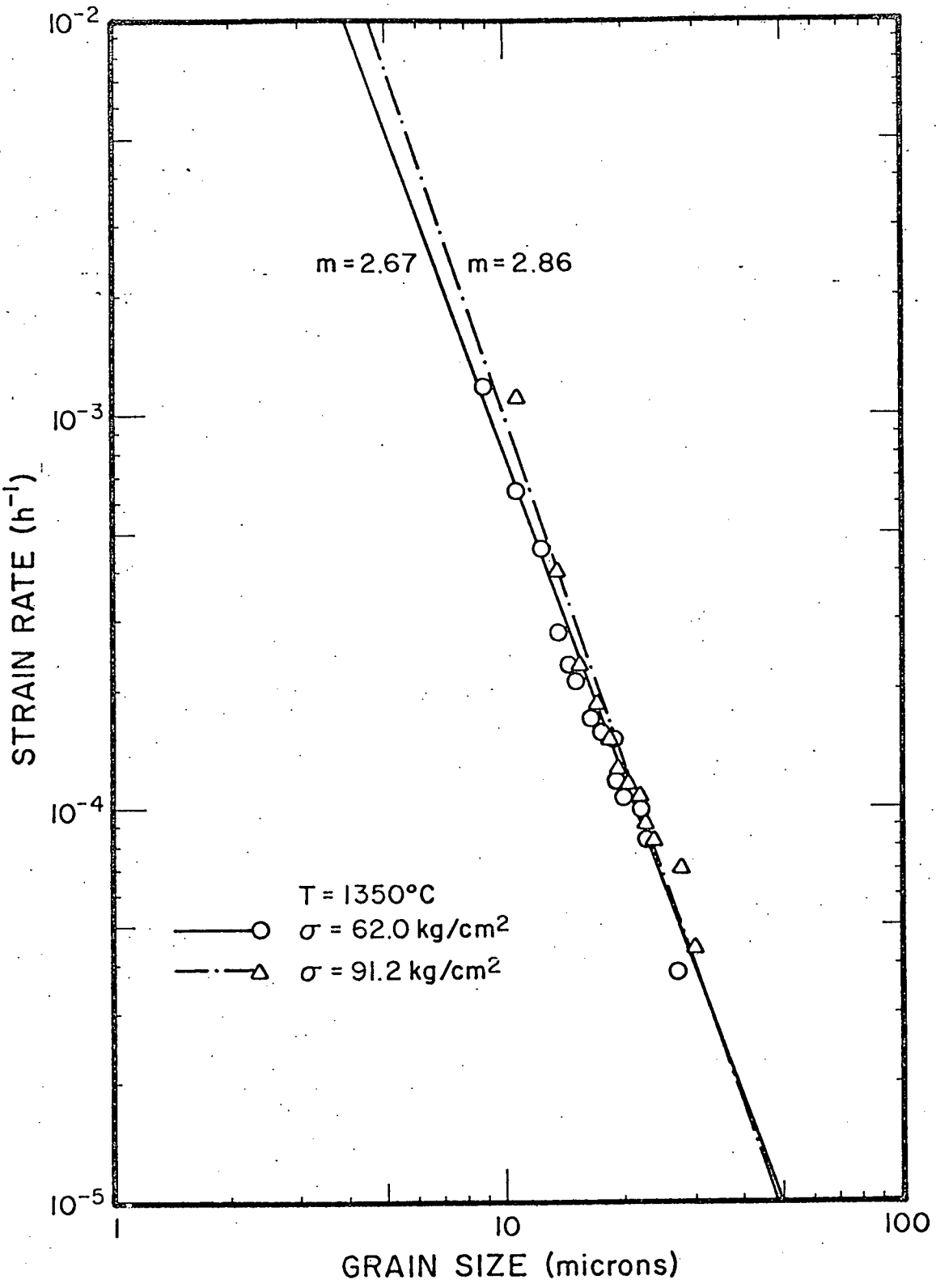

Figure 2 Effects of Grain Size on the Viscous Creep of Polycrystalline MgO Doped with 0.05 cation % Iron

reported some preliminary data which were insufficient for the evaluation of meaningful transport parameters. This year steady state creep rates were measured on various specimens doped with 5.3% iron over a range of grain sizes between 20 and 77 microns. These data at 1350°C are shown in Figure 3. Included in Figure 3 for comparison are the previous results at the 0.53 and 2.65% dopant levels. Least squares analyses of the data reveal grain size exponents m ($\dot{\varepsilon} \alpha (GS)^{-m}$) of 1.94, 2.38, and 2.38 for the 0.53, 2.65, and 5.3% dopant levels, respectively. A grain size exponent of 2.38 is indicative of a creep process in which mass transport by magnesium lattice diffusion (D^{ℓ}_{Mg}) and oxygen grain boundary diffusion ($\delta_0 D^{b}_{0}$) is comparable in magnitude. The creep rates (predicted) of the specimens at the 5.3% dopant level are 1.75 times faster than those at the 2.65% dopant level. Using the method developed by Gordon and Hodge [4], values of D^{ℓ}_{Mg} and $\delta_0 D^{b}_{0}$ were computed from the creep data in Figure 3. For the 5.3% dopant level, values of 1.51×10^{-11} cm^2/sec and 3.19×10^{-14} cm^3/sec were computed for D^{ℓ}_{Mg} and $\delta_0 D^{b}_{0}$, respectively at 1350°C. The significance of these calculations will be discussed in a subsequent section of this report.

2.1.3 Creep Activation Energies in Concentrated MgO-FeO-Fe_2O_3 Solid Solutions

In the creep regime (i.e. m = 2.38) observed in oxidizing atmospheres for heavily doped specimens (2.65 and 5.3%) apparent creep activation energies have been relatively low (~81 Kcal/mole) compared to the Nabarro-Herring regime (m ~ 2) in which the activation energy is much higher (~117 Kcal/mole). This low value has been attributed to oxygen grain boundary diffusion. However, the grain size exponents (2.38) are indicative of a process in which mass transport by oxygen grain boundary and magnesium lattice diffusion is

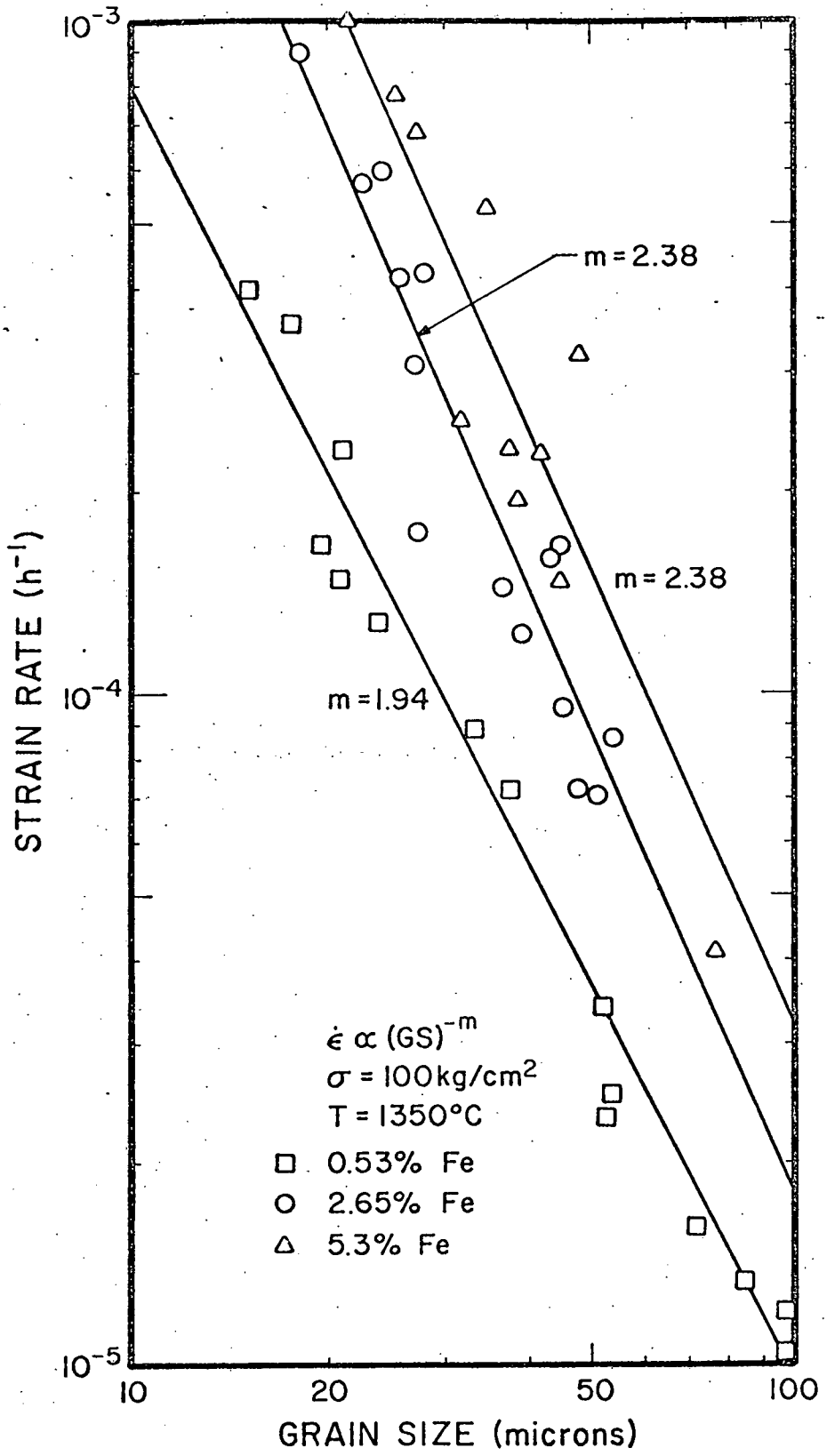

Figure 3 Effect of Grain Size on the Viscous Creep of Polycrystalline MgO Doped with 0.53, 2.65, and 5.3 cation % Iron

comparable in magnitude. Thus the activation energy of 81 Kcal/mole must be an over estimate for oxygen grain boundary diffusion, since it contains some contribution from magnesium lattice diffusion.

Using the ambipolar diffusional creep theory developed by Gordon [3,9], it can be shown that in this creep regime of mixed kinetics the creep rate is proportional to a "D complex", which in turn is related to D^{ℓ}_{Mg}, $\delta_0 D^{b}_{0}$, and the grain size (GS) by:

$$D_{complex} = \frac{D^{\ell}_{Mg}}{1 + \frac{(\frac{GS}{\pi})\, D^{\ell}_{Mg}}{\delta_0 D^{b}_{0}}} \qquad [1]$$

Since D^{ℓ}_{Mg} and $\delta_0 D^{b}_{0}$ are exponentially dependent in temperature the above equation can be expressed as:

$$D_{complex} = \frac{D_o \exp(-Q_1/RT)}{1 + \frac{(\frac{GS}{\pi})\, D_o \exp(-Q_1/RT)}{\delta_0 D'_0 \exp(-Q_2/RT)}} \qquad [2]$$

Q_1 and Q_2 are the activiation energies for magnesium lattice and oxygen boundary diffusion, respectively. Q_1 was assumed to be 117 Kcal/mole based on creep experiments in which cation lattice diffusion was found to be rate-controlling [8]. Q was estimated from oxygen tracer diffusion data [10] to be 56 Kcal/mole as an upper limit. Using these values and calculated diffusion coefficients (from creep data) for D^{ℓ}_{Mg} and $\delta_0 D^{b}_{0}$ at 1350°C, the pre-exponential terms (D_0, D'_0) were evaluated. A computer program was then used to generate values of $D_{complex}$ over a wide range of temperatures and grain sizes. The results of these calculations are summarized in Figure 4. The ambipolar model predicts a

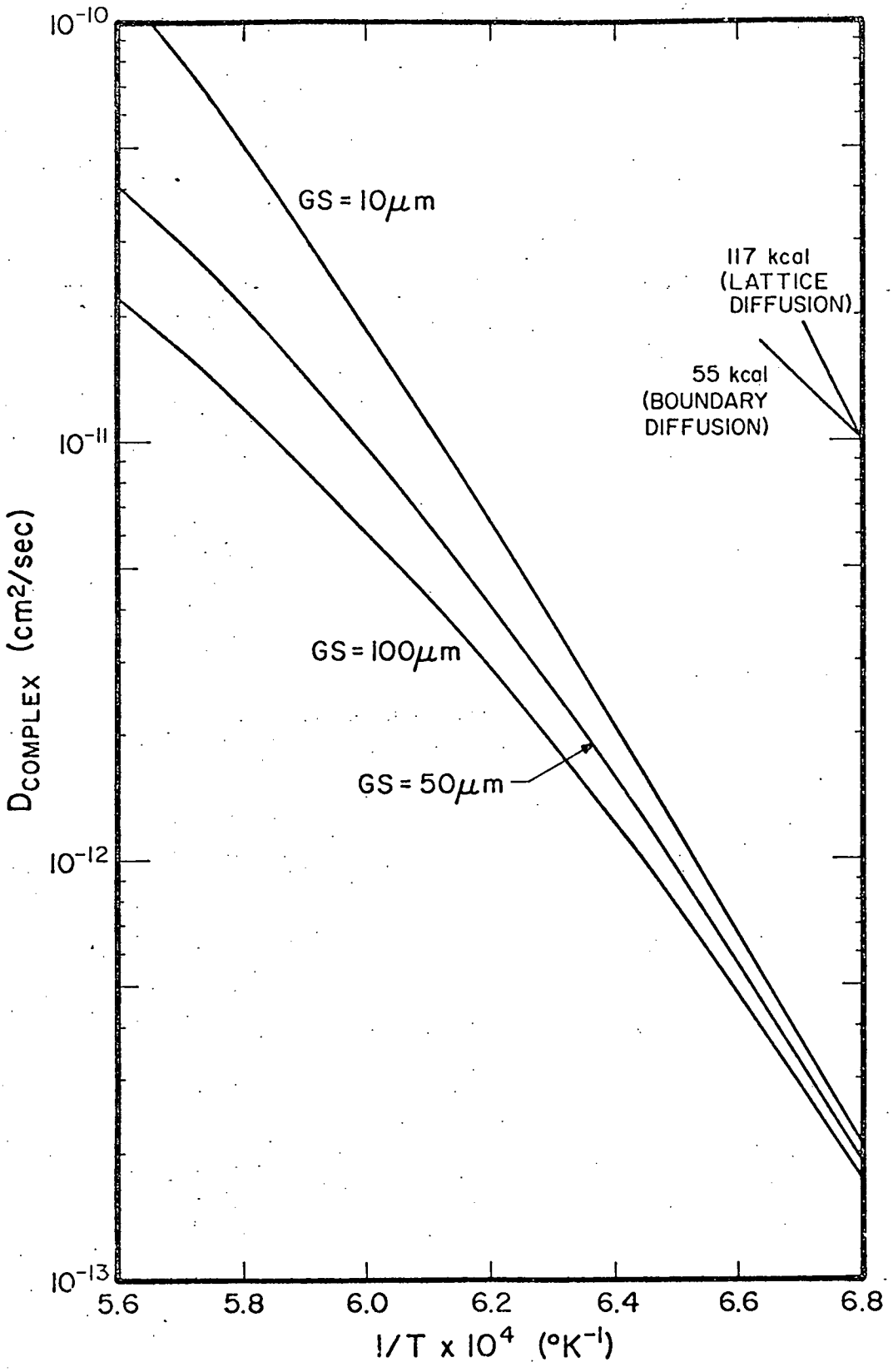

Figure 4 Computer Simulation of D Complex Versus Temperature

gradual decrease in activation energy as the temperature increases from 1200 to 1500°C. This variation in activation energy becomes more pronounced as the grain size is increased. At low temperatures magnesium lattice diffusion controls with an activation energy of ∿ 117 Kcal/mole. At higher temperatures, particularly large grain sizes, oxygen grain boundary diffusion begins to dominate and the activation energy drops.

To confirm these computer calculations, some experiments were conducted at two grain sizes (44 and 76μm) over the prescribed temperature range. The results of these experiments are shown in Figure 5. As can be seen from the data, a definite curvature exists in the activation energy plot with the most pronounced curvature present in the specimen with the largest grain size. At high temperatures (∿1500°C) the activation energy approached values around (66-74 Kcal/mole); at lower temperatures (∿1200°C) the activation energy was much higher (∿113 Kcal/mole). It is clear from these studies, a wide temperature range (>300°C) is required to separate the two processes of magnesium lattice and oxygen grain boundary diffusion. This is not always possible since excessive grain growth becomes a problem at high temperatures and creep rates become very slow at low temperatures.

2.1.4 Impurity Effects in Mass Transport Parameters in Polycrystalline MgO and MgO-FeO-Fe_2O_3 Solid Solutions

Enough diffusion values at various dopant levels have now been accumulated that we can begin to look at the effects of impurities on the revelent mass transport parameters for these systems. Values of D^{ℓ}_{Mg}, $\delta_O D^{b}_{O}$, and $\delta_{Mg} D^{b}_{Mg}$ at 1350°C are tabulated in Table 1. The effect of dopant concentration on D^{ℓ}_{Mg} is shown in Figure 6. It is clear that the magnesium lattice diffusion coefficient is a strong function of the iron concentration. Next year we will

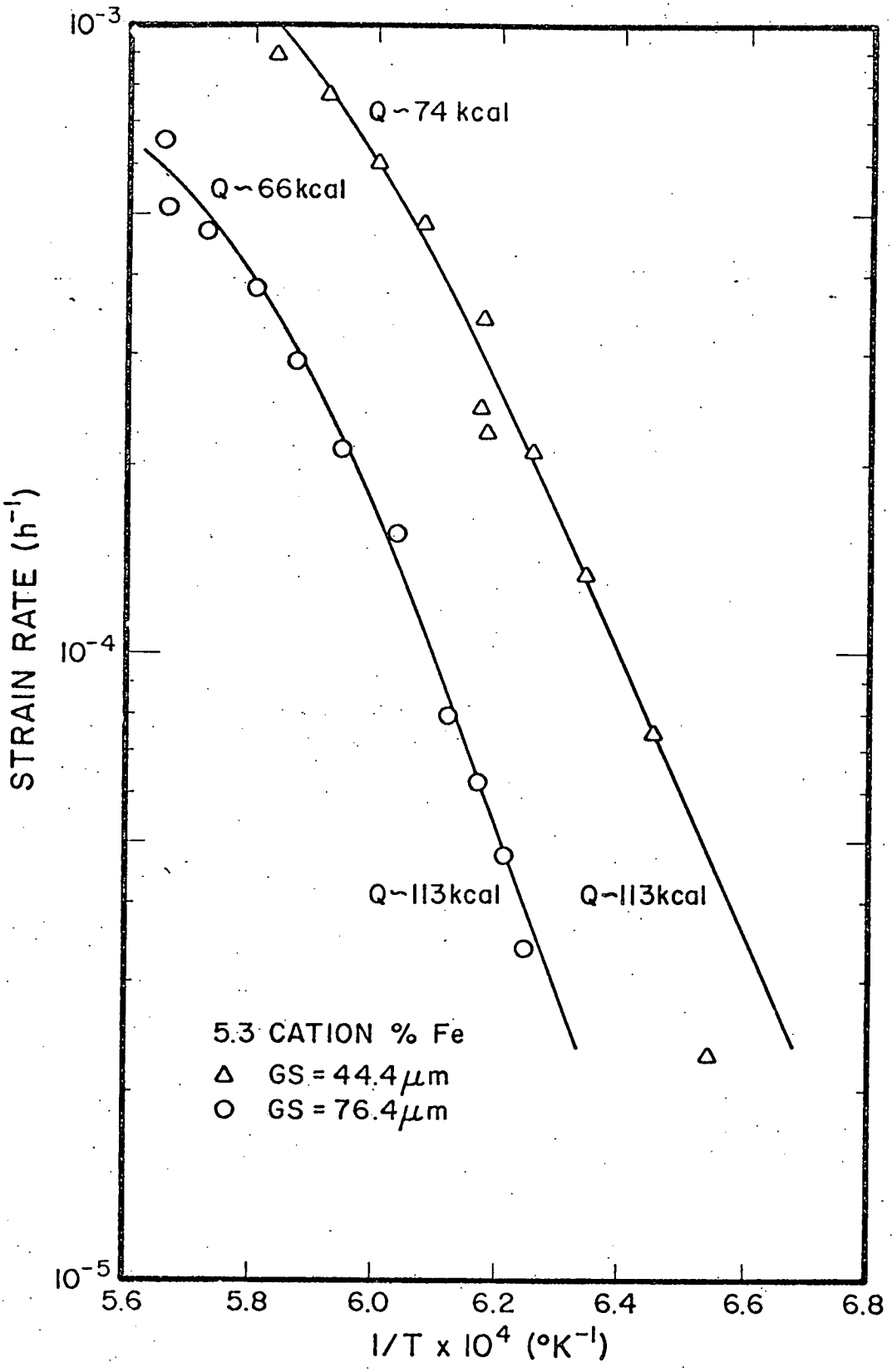

Figure 5 Effect of Temperature on the Creep of Polycrystalline MgO Doped with 5.3 cation % Iron

Table 1

Mass Transport Parameters in Polycrystalline MgO and MgO-FeO-Fe_2O_3 Solid Solutions

1350°C

Dopant Level (cation %)	D^{ℓ}_{Mg} (cm^2/sec)	$\delta_O D^b_O$ (cm^3/sec)	$\delta_{Mg} D^b_{Mg}$ (cm^3/sec)
Undoped*	1.5×10^{-12}	--	1.2×10^{-15}
0.05**	4.8×10^{-13}	--	7.3×10^{-16}***
0.53	2.3×10^{-12}	--	--
2.65	9.0×10^{-12}	1.6×10^{-14}	--
5.3	15.1×10^{-12}	3.2×10^{-12}	--
Magnesium Tracer	1.15×10^{-12}	--	--

*LiF used as a hot-pressing aid

**Average of two calculated values

***1.5×10^{-16} cm^3/sec and 1.5×10^{-17} cm^3/sec at 1300 and 1200°C, respectively as determined by Terwilliger, et al, (5,11)

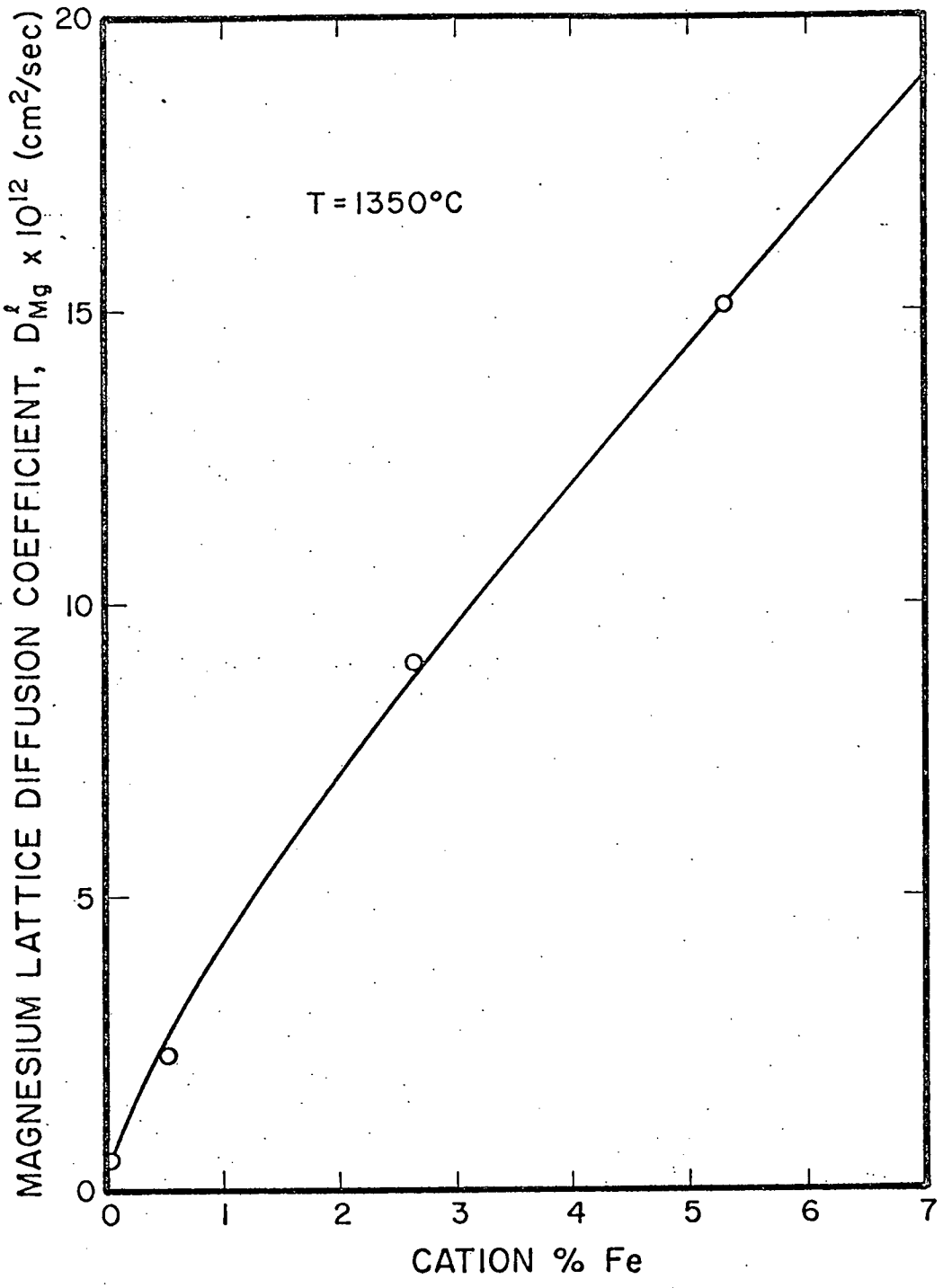

Figure 6 Effect of Iron Doping on Cation Lattice diffusion in MgO

determine the concentration of trivalent iron (and hence the concentration of cation lattice vacancies) at the various dopant levels to determine the dependence between D^{ℓ}_{Mg} and the concentration of lattice defects.

A contradiction exists between the mass transport parameters for the undoped and the 0.05% dopant level. D^{ℓ}_{Mg} for the undoped material is a factor of 3 larger than the 0.05% dopant level. This discrepancy could be due to one of two factors: (1) a slight contribution of non-viscous creep in the undoped material could give rise to overestimates of the diffusion parameters, (2) the pure MgO in this study was hot-pressed with LiF as an hot-pressing aid [6]. Recent auger analysis by Johnson et al., [12], reveals that significant amounts of F^- remains on the grain boundaries after fabrication. Any residual fluorine in the lattice could give rise to lattice vacancies and entranced cation diffusion. The creep tests on undoped MgO will be repeated next year on specimens prepared without the LiF additive.

2.2 Non-Viscous Creep of Polycrystalline MgO, Pure and Doped with Iron

Previously creep experiments have been extended into the regime of large grain sizes (136-487μm) for polycrystalline MgO, pure and doped with iron (0.53 cation %). Steady state, non-viscous creep was observed at temperatures between 1400 and 1500°C for stresses up to ∿400 kg/cm^2. The non-viscous stress exponents were in the range of 3.4 ± 0.5. Creep rates in this regime were found to be independent of grain size and, in the case of iron-doped material, independent of oxygen partial pressure. Creep rates were also insenstive to iron doping. These results are in marked contrast with the diffusional creep behavior in fine-grained material (<100 μm) tested at low stresses (<300 kg/cm^2). In the latter creep rates are very sensitive to changes in grain size, iron concentration, and oxygen partial pressure.

Stress exponents of approximately 3 and the absence of a grain size dependence strongly suggest the possibility of an intra-granular process involving dislocation climb as the dominant deformation mode in the non-viscous creep regime. Ample evidence exists from recent electron microscope studies in this and other [13,14] laboratories that dislocation activity is present. However, the lack of a P_{O_2} dependence and the insensitivity of the creep rate to iron doping suggest that the climb process is not diffusion controlled. This leaves open the possibility that interfacial processes (i.e. absorption or desorption of defects at dislocations) or dislocation core diffusion are rate determining in the non-viscous creep regime.

Additional experiments were conducted this year by the method of stress relaxation under conditions of four point bending to determine the creep characteristics of pure and iron-doped polycrystalline MgO over a wide range of stress (up to ∿1000 kg/cm^2). In Figure 7, stress relaxation

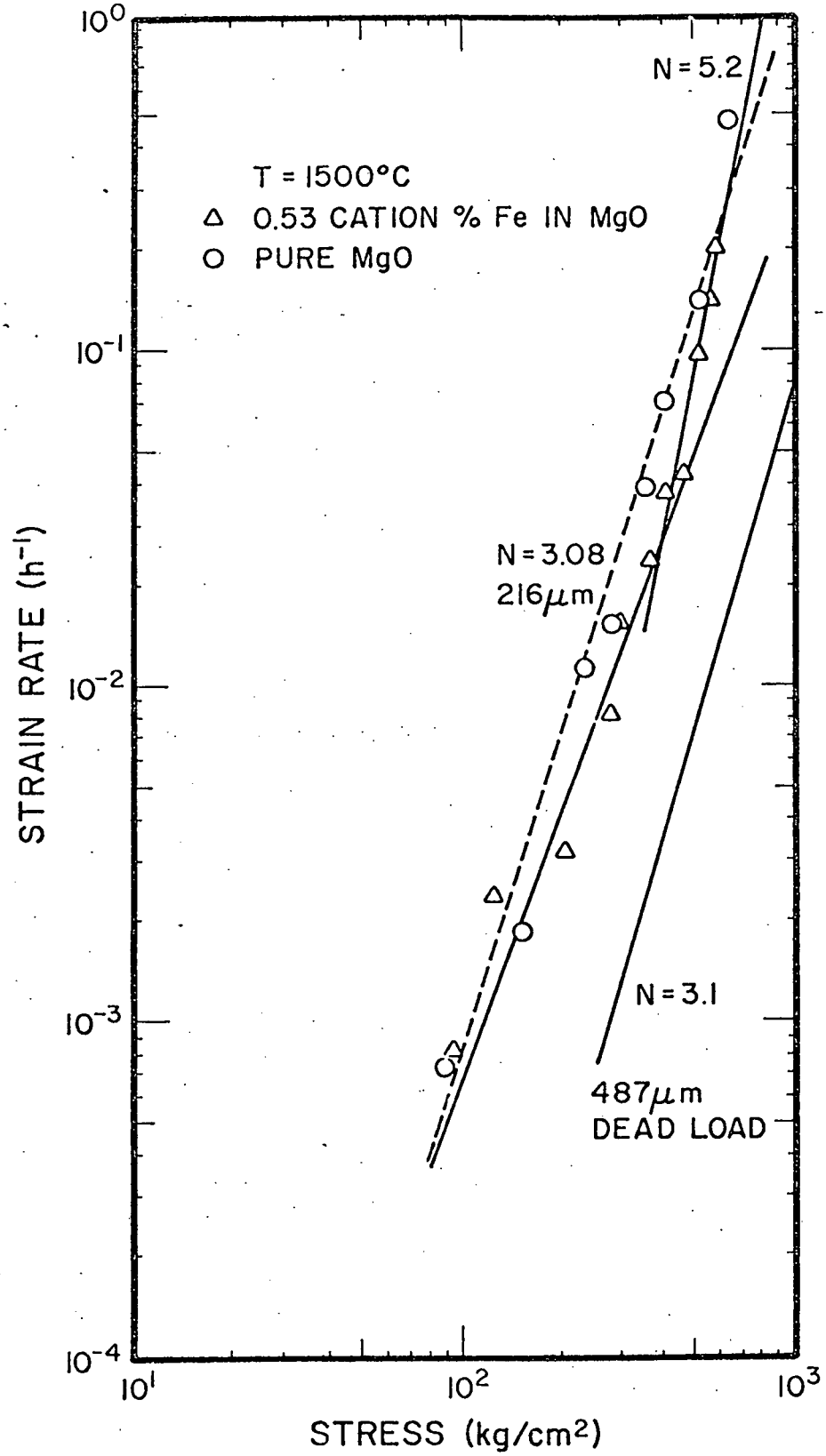

Figure 7 Stress Relaxation at 1500°C in Polycrystalline MgO, Pure and Doped with 0.53 cation % Iron

tests are shown for coarse-grained (216-487 μm) MgO, pure and doped with iron (0.53% cation %). Reproducible stress relaxation curves were measured after the third loading in the doped material and after the 19th loading in the undoped oxide. Stress relaxation curves, which are reproducible with repeated loadings, are taken as an indication of a steady state structure and thus comparable to creep curves obtained from dead-load creep tests under conditions of steady state creep. As can be seen from Figure 7, stress exponents around 3 (at stresses $\leq$ 400 kg/cm^2) were measured. These are in good agreement with those measured in dead-load tests over a similar range of stress. Also, the creep rates of the undoped material are only slightly faster than those measured in the doped oxide.

In these particular experiments, load point instead of center point deflections were measured. This procedure introduces an overestimation of the strain rate by a factor of 8 to 10. Thus the agreement between the dead-load and stress relaxation data, when the compliance error is taken into account, is reasonable.

Finally, a stress relaxation test using center point deflections was conducted on a fine-grained (25 μm) iron doped specimen at 1350°C to (1) determine the transition between viscous and non-viscous creep and (2) to compare magnitudes of creep rates with dead-load creep data. The results of these tests, shown in Figure 8, indicate a sharp transition between viscous creep ($N \approx 1$) to power law creep at a stress of 160 kg/cm^2. Viscous behavior has been documented up to stresses around 300 kg/cm^2 in dead-load creep tests [8]. The agreement with the dead-load data is considered to be reasonable. It is clear that stress relaxation tests can be used effectively to (1) measure high creep rates ($\sim 1h^{-1}$) at high stresses

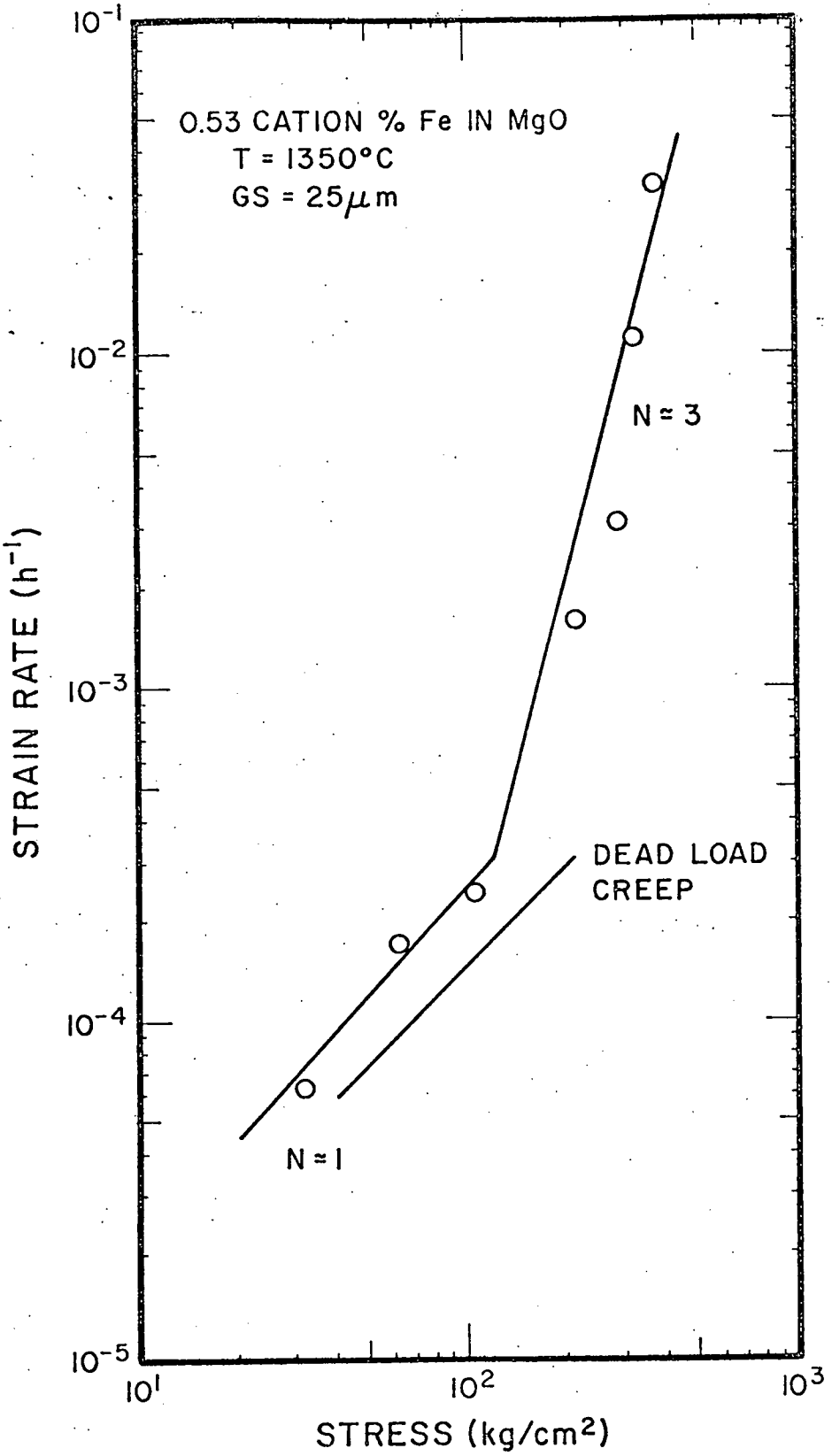

Figure 8 Stress Relaxation at 1350°C in Polycrystalline MgO, Doped with 0.53 cation % Iron

($\sim$ 1000 kg/cm^2) and (2) determine transitions between viscous and power law creep regimes. Since these experiments are conducted approximately under conditions of constant plastic strain, experimental problems in dead-load testing at high strain rates and stresses associated with extensive deformation and fracture are avoided.

2.3 Dead-Load Creep of Polycrystalline Alumina, Pure and Doped with Transition Metal Impurities

Now that much of the work on the effects of stress, grain size, and temperature on the steady state creep rate under dead-load conditions has been completed, it is appropriate to bring all of the work accomplished to date into proper perspective.

2.3.1 Stress Dependence of Steady State Creep Rate

A major objective of this study was to document the strain rate-stress dependence for the creep of pure and doped polycrystalline Al_2O_3 over a wide range of experimental conditions. In the course of this contract, a large amount of data has been accumulated on pure and doped (Fe, Cr, Ti-Mn) material over a range of temperatures (1100-1550°C), grain sizes (6-1200 μm), dopant levels (up to 2 cation %), and oxygen partial pressures (0.86-10^{-9} atm) in an effort to distinguish creep regimes in which viscous (i.e. $\dot{\varepsilon} \alpha \sigma^N$, N = 1), slightly non-viscous (N = 1.1 - 1.7), and non-viscous (N > 1.7) behavior is dominant.

Reports of slightly non-viscous creep of polycrystalline Al_2O_3 abound in the literature. Heuer, et al, [15] were the first investigators to document this behavior. They reported stress exponents N between 1.08 and 1.67 for bending tests on pure and MgO-doped Al_2O_3 (1.8 < G.S. < 16.5 μm; 1300 $\leq$ T $\leq$ 1700°C) at stresses between 70 and 2114 kg/cm^2. These authors also reanalyzed the earlier work of Folweiler [16] and concluded that stress exponents ranging between 1.07 and 1.7 were more represenative of the creep data than viscous

behavior (N = 1). Later Cannon [17] and Sugita and Pask [18] reported slightly non-viscous behavior (N = 1.1 - 1.3) for the compression creep testing of MgO-doped, polycrystalline Al_2O_3 .

A summary of stress exponents measured during the course of the contract is given in Table 2. In general, nearly all of the creep data are characterized by slightly non-viscous creep behavior with stress exponents that vary between 1.03 and 1.43 for grain sizes between approximately 6 and 110 μm. Two interesting and notable exceptions of viscous creep (N = 1) have been observed in this small grain size range for doped polycrystalline Al_2O_3: (1) double dopant of 1/4% Mn and 1/4% Ti and (2) 2% Fe at an oxygen partial pressure of $\sim 10^{-7}$ atm. In both of these systems, truly viscous behavior, as represented by a linear relationship between the creep rate and stress (refer to Figure 9 for representative examples), was found to be coincident with a reciprocal grain size dependence consistent with a process controlled by oxygen grain boundary diffusion.

Larger stress exponents (1.4 - 1.8) were found in creep tests at 1450°C in pure and chromium-doped specimens with larger grain sizes (70-306 μm). When similar specimens were tested at higher temperatures (1550°C), significantly non-viscous behavior (N = 2.3 - 2.9) was encountered and is similar to that reported earlier in the literature.

2.3.2 Grain Size Effects on the Steady State Creep Rate

The preliminary data which were reported last year (6) for pure, chromium-doped and iron-doped polycrystalline Al_2O_3 have been supplemented with additional data. Furthermore, grain size effects have been determined for specimens doped with the double dopant (1/4% Mn + 1/4% Ti).

All of the grain size data to date are summarized in Figure 10 for a range of grain size between 6 and 100 μm and for creep tests at 1450°C in the regime of low stress (50 kg/cm^2) where viscous behavior is expected to be dominant.

Table 2

Strain Rate-Stress Exponents (N) in Polycrystalline Al_2O_3

Composition (cation %)	N	Grain Size (μm)	Temperature (°C)	Stress (kg/cm²)	P_{O_2} (atm)	Number Specimens
Undoped	1.30 ± 0.15	9-72	1450	40-500	0.86	5
Undoped	1.76	76	1450	30-300	0.18	1
Undoped	1.40	306	1450	40-100	0.18	1
Undoped	2.88	306	1550	40-100	0.18	1
Undoped	2.33	306	1550	40-200	0.18	1
1% Cr	1.30	9	1400-1500	50-550	0.86	2
1% Cr	1.03	15	1450	40-500	0.86	1
1% Cr	1.21	32	1450	40-500	0.86	1
1% Cr	1.43	77	1450	40-320	0.86	1
1% Cr	1.67	276	1450	40-90	0.86	1
10% Cr	1.15 ± 0.04	6	1450	40-400	10^{-9}	2
10% Cr	1.11	29	1450	40-100	10^{-9}	1
10% Cr	1.48	60	1450	40-200	0.86	1
10% Cr	2.38	1200	1550	80-290	0.86	1
0.2% Fe	1.14 ± 0.06	15	1400-1500	10-100	0.86	3
0.2% Fe	1.14	27-38	1450	40-500	0.86	2

Table 2 (continued)

Composition (cation %)	N	Grain Size (μm)	Temperature (°C)	Stress (kg/cm²)	P_{O_2} (atm)	Number Specimens
1.0% Fe	1.0	15	1500	10-150	0.86	1
1.0% Fe	1.25 ± 0.06	26-107	1450	40-500	0.86	3
1.0% Fe	1.25 ± 0.05	42	1400-1500	50-550	0.86	1
1.0% Fe	1.0	15	1500	10-100	6.31×10^{-3}	1
1.0% Fe	1.29	38	1450	40-500	10^{-8}	1
2.0% Fe	1.05	28	1450	40-360	10^{-6}	1
2.0% Fe	1.03	28	1450	40-340	10^{-6}	1
2.0% Fe	0.90	28	1250	40-300	10^{-6}	1
1/2% Ti	1.30	63	1525	10-100	0.86	1
1/2% Ti	1.07	63	1525	30-300	10^{-9}	1
1/4% Ti - 1/4% Mn	0.79	24	1100	40-200	0.86	1
1/4% Ti - 1/4% Mn	1.00	30	1300	40-400	0.86	1
1/4% Ti - 1/4% Mn	1.04	38	1300	80-400	0.86	1
1/4% Ti - 1/4% Mn	0.80	40	1250	40-200	0.86	1

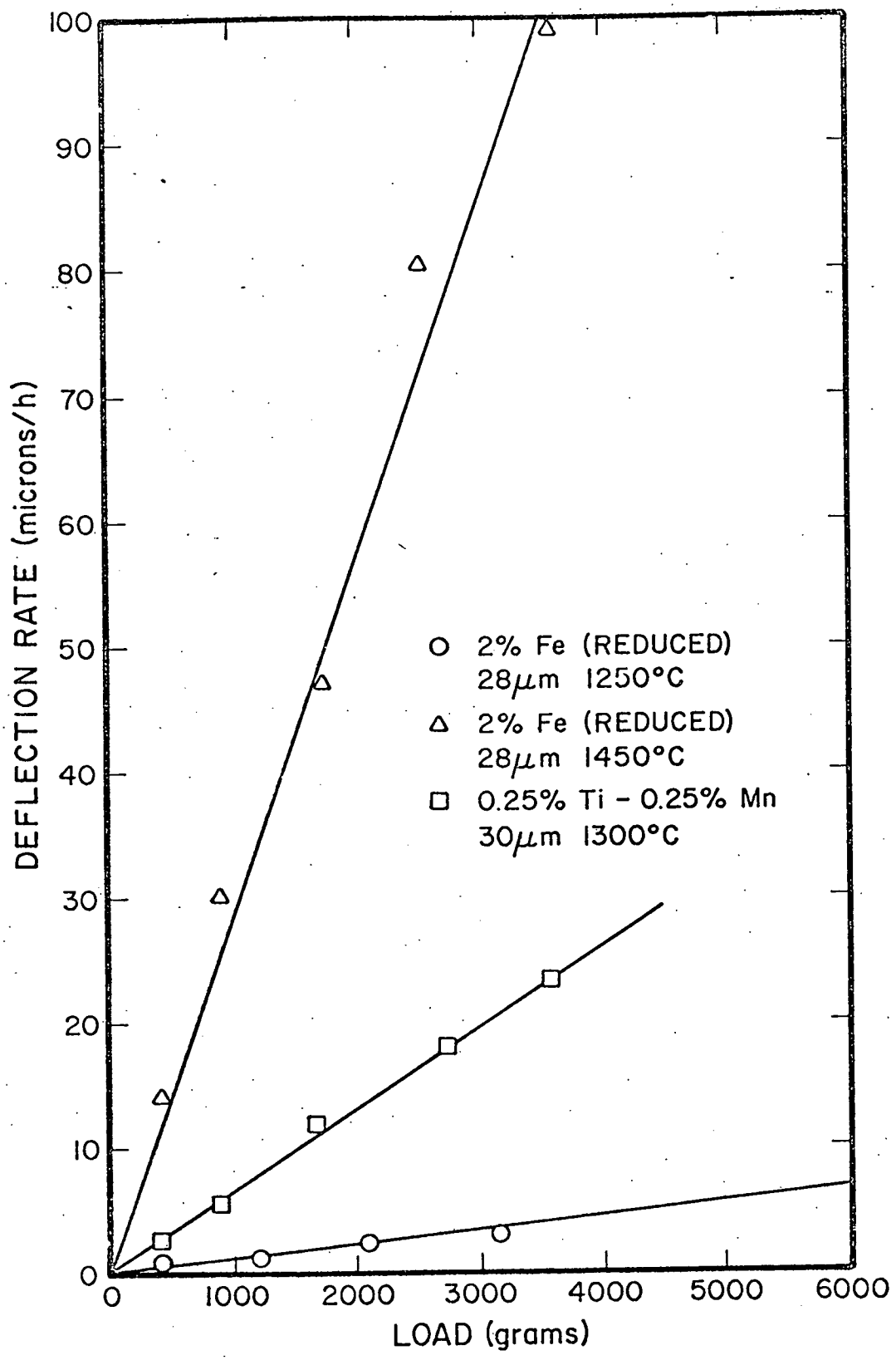

Figure 9 Viscous Creep of Polycrystalline Al_2O_3 Doped with 2% Iron ($P_{O_2} \sim 10^{-7}$ atm) and 1/4% Mn - 1/4% Ti

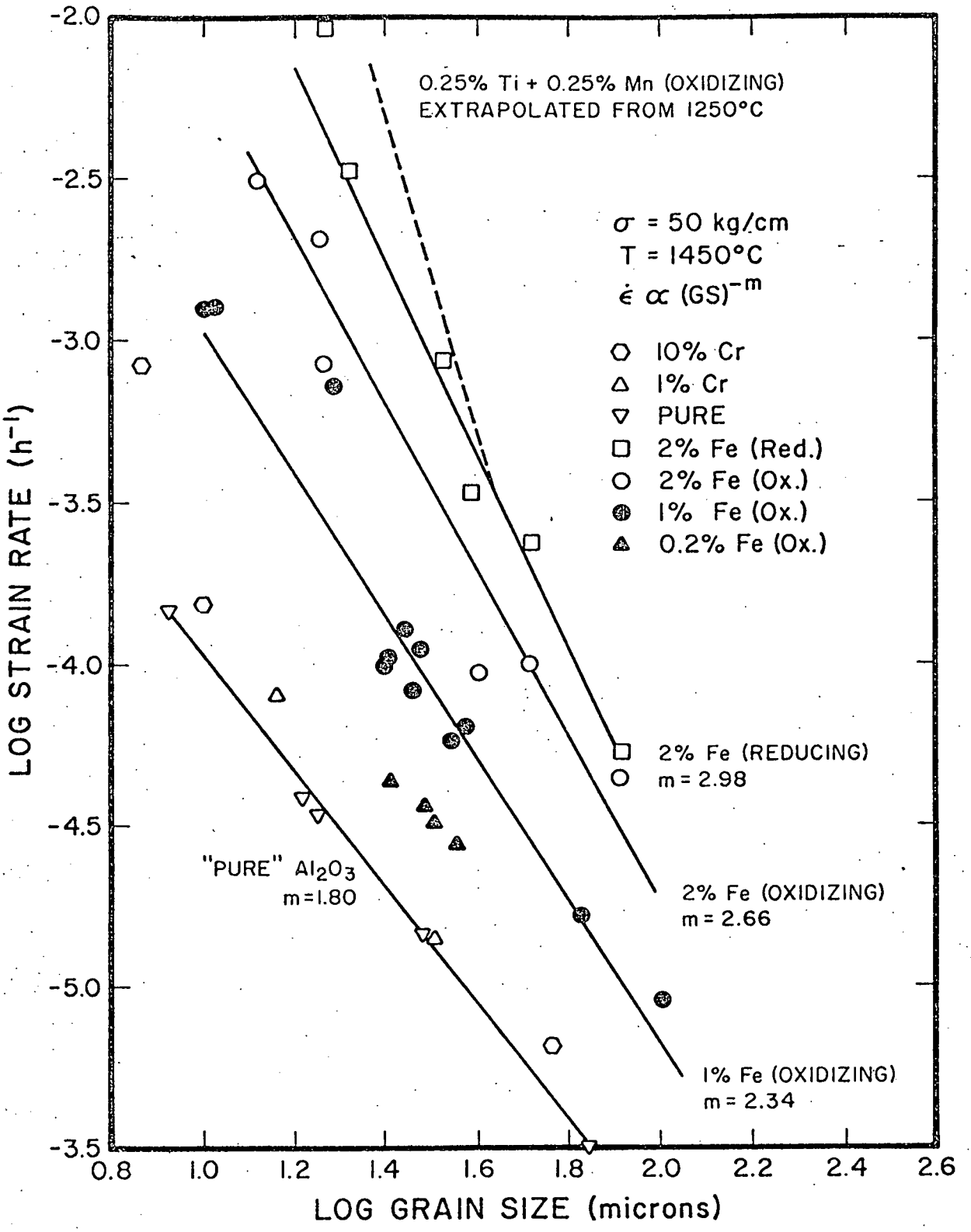

Figure 10 Grain Size and Impurity Effects on the Creep of Polycrystalline Al_2O_3

Chromium additions up to 10% have essentially no effect on the creep rate of polycrystalline Al_2O_3 in the low stress and small grain size regimes. Least squares analyses of the data revealed grain size exponents m ($\dot{\varepsilon} \alpha (GS)^{-m}$) of 1.80 for pure Al_2O_3, 2.13 for both the 1 and 10% Cr specimens combined, and 2.07 for all the pure and chromium-doped materials combined. These data are consistent with the interpretation that the steady state creep rate is controlled by a cation lattice diffusion process (i.e. Nabarro-Herring creep).

Included in Figure 10, for comparison, are creep data for iron-doped polycrystalline Al_2O_3 over a range of impurity concentrations (0.2 - 2%). In creep tests conducted in air and in reducing atmospheres ($\sim 10^{-7}$ atm), it is expected that a significant fraction of the iron is present as a divalent ion in substitutional solid solution for aluminum. Additions of 0.2, 1.0, and 2.0 cation % iron enhanced the creep rate of polycrystalline Al_2O_3 by factors of $\sim$2, $\sim$7, and $\sim$18 respectively. Reducing the oxygen partial pressure from 0.86 to 4.66 x 10^{-7} atm increased further the creep rate of the specimens doped with 2% Fe. All of these results, in combination with the effects of P_{O_2} reported earlier by Hollenberg and Gordon [19], indicate that divalent iron enhances the diffusional creep rate of polycrystalline Al_2O_3. Specimens doped with the double dopant (Mn - Ti) in which the titanium is probably quadrivalent and the manganese is divalent possessed creep rates comparable in magnitude to material doped with 2% Fe and creep tested in a reducing environment. The creep rate of specimens doped with the double dopant was insensitive to changes in oxygen partial pressure (0.86 - 10^{-9} atm.).

Gordon [3] has predicted for the system Al_2O_3-Fe_2O_3-FeO in the limit of a large grain size and/or a high value of the aluminum ion lattice diffusivity (D_{Al}^{ℓ}), that the diffusional creep rates in the low stress regime will be rate controlled by oxygen grain boundary diffusion (because cation lattice diffusion becomes too rapid). Aluminum lattice diffusion can be

enhanced by increasing the iron dopant level and/or reducing the oxygen partial pressure. Both of these changes will increase the concentration of divalent iron leading to enhanced lattice diffusion via aluminum ion interstitials.

Verification of Gordon's predictions are shown in Figure 10. Doping with 1% Fe not only increased the creep rate in air but also modifed the grain size dependence from a grain size exponent (m) of ~2 to 2.34. An exponent of 2.34 is intermediate to that expected by the Nabarro-Herring (m = 2) and Coble (m = 3) theories for lattice and grain boundary diffusion control of the creep rate. Using a procedure developed by Gordon and Hodge [4] for the creep of polycrystalline MgO, aluminum lattice (D_{Al}^{ℓ}) and oxygen grain boundary ($\delta_0 D_0^b$) diffusion coefficients can be extracted from the creep data. When both cation lattice and anion grain boundary diffusion contribute to the overall creep rate, the respective diffusion coefficient can be computed from the following equation:

$$\dot{\varepsilon} = \frac{44\Omega_v\sigma}{2\pi\ kT\ (GS)^2} \quad \frac{D_{Al}^{\ell}}{1 + \frac{3}{2}\ \frac{(GS)\ D_{Al}^{\ell}}{\pi\delta_0 D_0^b}} \qquad [3]$$

Under these conditions, the creep rate will exhibit a mixed grain size dependence ($2 < m < 3$). Equation [3] can be rewritten in the form:

$$\dot{\varepsilon}\ (GS)^2 = -\frac{3}{2\pi}\frac{D_{Al}^{\ell}}{\delta_0 D_0^b}\ \dot{\varepsilon}(GS)^3 + \frac{44}{\pi}\frac{\Omega_v\sigma}{kT}\frac{D_{Al}^{\ell}}{2} \qquad [4]$$

In equations [3] and [4] Ω_v is the molecular volume of Al_2O_3, σ is the stress, GS is the grain size, T is the absolute temperature, k is Boltzmann's constant, D_{Al}^{ℓ} is the aluminum lattice diffusion coefficient, D_0^b is the oxygen grain boundary diffusion coefficient, and δ_0 is the effective griain boundary thickness for oxygen grain boundary diffusion. Referring to equation [4], a

a plot of $\dot{\varepsilon}_\ell (GS)^2$ versus $\dot{\varepsilon}_\ell (GS)^3$ yields a line of slope equal to $\left[-\frac{3}{2\pi}\frac{D^\ell_{Al}}{\delta_0 D^b_0}\right]$ and intercept equal to $\left[\frac{44}{\pi}\frac{\Omega_v \sigma}{kT}\frac{D^\ell_{Al}}{2}\right]$. Using predicted points from the least squares line in Figure 10, values for D^ℓ_{Al} (6.72×10^{-12} cm^2/sec) and $\delta_0 D^b_0$ (2.10×10^{-14} cm^3/sec) were calculated for polycrystalline Al_2O_3 doped with 1% Fe (equilibrated in an air atmosphere).

By doping at even higher concentrations (i.e. 2 cation % Fe) and reducing the oxygen partial pressure (4.66×10^{-7} atm) D^ℓ_{Al} can be increased even further at 1450°C without the precipitation of a second phase. If Gordon's ambipolar diffusional creep theory is correct, these changes should lead to larger grain size exponents (m) and creep rates controlled more and more by oxygen grain boundary transport. As indicated in Figure 10, doping with 2% Fe and creep testing in air resulted in higher strain rates and a larger grain size exponent (m = 2.66). When creep tests were conducted in a reducing atmosphere ($P_{O_2} = 4.66 \times 10^{-7}$ atm.), creep rates increased even further, the relative increase was smaller at large grain sizes than in fine-grained material. Under these conditions the creep grain size exponent was 2.98, its largest value and in excellent agreement with that predicted by Coble creep.

In Table 3, a summary is given for values of D^ℓ_{Al} and $\delta_0 D^b_0$ computed from creep data at the 0.0, 0.2, 1.0 and 2.0% dopant concentrations. The data in Table 3 indicate that both D^ℓ_{Al} and $\delta_0 D^b_0$ increase with iron doping, in particular the concentration of divalent iron. In addition as D^ℓ_{Al} increases the relative contribution of oxygen grain boundary diffusion increases giving rise to increasing values of the creep rate grain size exponent. Both of these effects are in accord with that predicted by the ambipolar diffusional creep theory of Gordon. [3,9]

Table 3

Cation Lattice and Anion Grain Boundary Diffusivities (1450°C) in Iron-Doped, Polycrystalline Al_2O_3

P_{O_2} (atm)	Cation % Fe	D_{Al}^{ℓ} (cm^2/sec)	$\delta_O D_O^b$ (cm^3/sec)	m
0.18	0*	6.9×10^{-13}	-	~2
0.18	0.2*	1.7×10^{-12}	-	~2
0.18	1.0**	6.7×10^{-12}	2.1×10^{-14}	2.34
0.18	2.0**	5.0×10^{-11}	4.1×10^{-14}	2.66
4.66×10^{-7}	2.0***	-	5.9×10^{-14}	2.98
Tracer (Extrapolated)		1.0×10^{-13}		

*Calculated from Nabarro-Herring creep equation modified for an ionic compound (3)

**Calculated by a procedure similar to that reported by Gordon (3) and Gordon and Hodge (4)

***Calculated from Coble creep equation modified for an ionic compound (3)

The effect of grain size on the creep rate of polycrystalline Al_2O_3 doped with both 1/4% Mn and 1/4% Ti is shown in Figure 11 for steady state creep experiments at 1250°C. A least squares analysis of the data indicates a very strong grain size dependence ($\dot{\varepsilon} \alpha (GS)^{-m}$; m=4.4). A grain size exponent of 4.4 is larger than that predicted by the Coble creep equation (m = 3). However, the least squares line is strongly influenced by the rates at the two smallest grain sizes. These could be artificially high due to transient effects. In any case the data give a grain size dependence which is consistent with creep rates controlled by oxygen grain boundary diffusion.

Extrapolation of these results from 1250 to 1450°C in Figure 10 indicated that the creep rates of alumina doped with 1/4% Mn and 1/4% Ti were comparable to the creep rate of material doped with 2% Fe which was tested in a reducing atmosphere to promote most of the iron into the divalent state. To confirm this extropolation, a specimen doped with 2% Fe was creep tested at 1250°C in a reducing atmosphere. The resulting creep rate was in excellent agreement with those in Figure 11 for the double dopant. Thus it can be concluded that polycrystalline Al_2O_3 which is doped with either 1/4% Mn and 1/4% Ti or 2% Fe (in a reduced state) possesses equivalent creep characteristics: (1) creep rates are comparable, (2) the grain size effects are consistent with creep rates controlled by oxygen grain boundary diffusion, (3) viscous creep behavior is exhibited in both cases. The mixed dopant (Mn-Ti) evidently is much more efficient in creating lattice defects than is iron at the 2% dopant level under reducing conditions. The enchancement of the creep rate by the double dopant is believed to be due to impurities in solid solution because of the following observations: (1) No second phase was observed in polished sections. Lattice parameter measurements for the mixed dopant reveal essentially

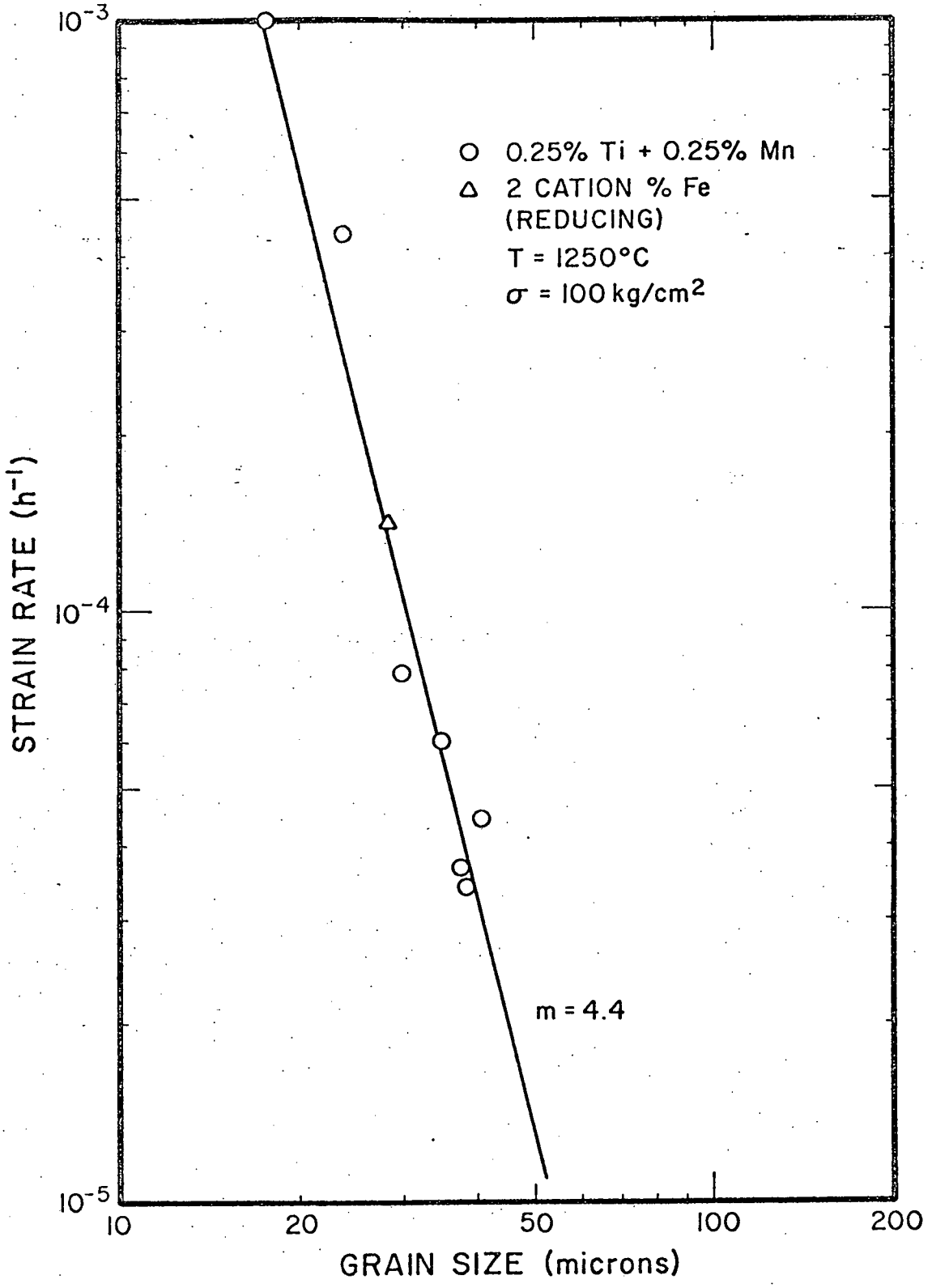

Figure 11 Grain Size Dependence of Polycrystalline Al_2O Doped with 1/4% Ti and 1/4% Mn

no change from pure Al_2O_3. (2) Scanning electron microscope (EDAX) x-ray scans for impurity segregation in grain boundaries (fracture surfaces) as compared to polished sections (bulk material) revealed no difference in Mn and/or Ti concentrations. (3) Temperature excursions between 1000 and 1300°C indicate no sharp transitions in the creep rate which might be indicative of liquid phase formation.

Finally, it is interesting to note that when the creep process is rate-controlled by oxygen grain boundary diffusion (1/4 Mn - 1/4 Ti and 2% Fe - reducing), the creep rate is linear with the stress (viscous creep). Since the creep of polycrystalline is normally slightly non-viscous when there is a contribution of both cation lattice and anion grain boundary diffusion, there is an indication that the non-viscous behavior is associated with the bulk diffusion of the cation.

2.3.3 Activation Energy for the Creep of Pure and Transition Metal Doped Polycrystalline Al_2O_3

Creep activation energies were determined from temperature change experiments (1350 - 1525°C) on pure, chromium-doped, and iron-doped polycrystalline Al_2O_3. Comparable tests were conducted on specimens with the double dopant (Mn - Ti) at temperatures between 1000 and 1250°C. A summary of all activation energies is given in Table 4. An activation energy of approximately 129 Kcal/mole is characteristic of deformation in pure and chromium-doped alumina. For the specimens doped with 1 cation % Fe, in which the deformation made was a mixture of both cation lattice and anion boundary diffusion, values ranged between 143 Kcal/mole on the high end to a lower limit of 117 Kcal/mole. Finally the activation energies for specimens in which the deformation mode was controlled entirely by anion grain boundary diffusion ranged between 94 and 119 Kcal/mole on the low end of the experimental range.

In the diffusional creep of a polycrystalline material in which cation lattice diffusion is comparable to anion grain boundary diffusion (e.g. 1% Fe in air), the apparent creep activation energy is expected to vary both with temperature and grain size because of the dependence between the complex diffusion coefficient ($D_{complex}$), the grain size, the cation lattice diffusion coefficient, and the anion grain boundary diffusion coefficient according to the following relations:

$$\dot{\varepsilon} = \frac{44\Omega_v\sigma}{kT\,(GS)^3}\, D_{complex} \qquad [5]$$

$$D_{complex} = \frac{\frac{1}{2}\left[\frac{(GS)}{\pi} D^{\ell}_{Al}\right]}{1 + \frac{3}{2}\,\frac{(GS)}{\pi}\,\frac{D^{\ell}_{Al}}{\delta_0 D^{b}_{0}}} \qquad [6]$$

If activation energies of 150 and 105 Kcal/mole are assigned, respectively, to

Table 4

Summary of Creep Activation Energies for Polycrystalline Alumina, Pure and Doped with Transition Metal Impurities

Dopant	No. of Specimens	Activation Energy (Kcal/mole)	Grain size (μm)	Grain Size Exponent (m)
Undoped	2	130 ± 5	18	1.80
1% Cr	1	124	15	∿2
1% Cr	1	129	30	∿2
0.2% Fe	1	134	25	∿2
1% Fe	1	115	15	2.34
1% Fe*	1	143	15	-
1% Fe	1	125	32	2.34
1% Fe	1	117	66	2.34
1% Fe	1	117	107	2.34
2% Fe (Reducing)	1	119	81	2.98
1/4 Ti - 1/4 Mn	1	100	24	4.4
1/4 Ti - 1/4 Cu**	1	94	15	>3

*From earlier work by Hollenberg and Gordon [19]

**Comparable creep rates with the Ti - Mn mixed dopant; grain size effects assumed to be similar

aluminum lattice diffusion and oxygen grain boundary diffusion in iron-doped Al_2O_3, then the apparent activation energy at 1450°C would vary between 140 Kcal/mole at a grain size of 16μm to 120 Kcal/mole at a grain size of ∿120μm. This range is comparable to that observed experimentally. The highest activation (∿150 Kcal/mole) energy would be expected in fine-grained samples (<1μm) tested at low temperatures (∿1200°C) while the lowest activation energy would occur in large grain size (>120μm) material tested at high temperatures (>1600°C). When one considers that creep activation energies have an experimental uncertainty of ± 10 Kcal/mole, a maximum variation in the apparent activation energy of approximately 20 Kcal/mole would be difficult to distinguish in the realm of experimental grain sizes (6 - 110μm) and temperatures where dead-load creep rates are readily measured (1400 - 1600°C).

2.3.4 Estimation of Diffusion Coefficients from Diffusional Creep Data

Aluminum lattice diffusion coefficients in polycrystalline Al_2O_3, pure and doped with chromium and iron are plotted at various temperatures in Figure 12 using the data in Tables 3 and 4. In all cases the diffusion coefficients are larger than those obtained from an extropolation of aluminum tracer values at higher temperatures. It should be noted that all computations of diffusivities were made using creep data in the limit of low stress (50 kg/cm^2). Consequently, it is not likely that the diffusivities are overestimated because of the slightly non-viscous behavior which becomes an important factor at higher stress levels.

The effect of iron doping on cation lattice diffusion is readily apparent. Nearly two orders of magnitude ($\sim$70 X) separate the diffusion coefficients for pure Al_2O_3 and material doped with 2% Fe.

Included also in Figure 12 are values of D^{ℓ}_{Al} computed from the viscous creep of polycrystalline Al_2O_3 saturated with MgO. In a composite analysis of eight different creep studies, Cannon and Coble (20) report that all the data fall within a factor of two of the following expressions:

$$D^{\ell}_{Al} = 1.36 \times 10^5 \exp\left(-\frac{138{,}000}{RT}\right) \quad cm^2/sec$$

These values are in resonable agreement with the values estimated from the undoped and chromium-doped specimens from this study.

As the concentration of cation lattice defects increase by either doping with divalent iron or the double dopant (Mn - Ti) cation lattice diffusion increases to a level at which it is too fast to be rate controlling. At this stage, the creep rate becomes rate limited by oxygen grain boundary diffusion. Estimates of $\delta_0 D^b_0$ inferred from the creep of polycrystalline Al_2O_3 doped with 1% Fe (oxidizing), 2% Fe (oxidizing and reducing), and 0.25% Ti - 0.25% Mn (oxidizing and reducing) are shown in Figure 13. Included for comparison are

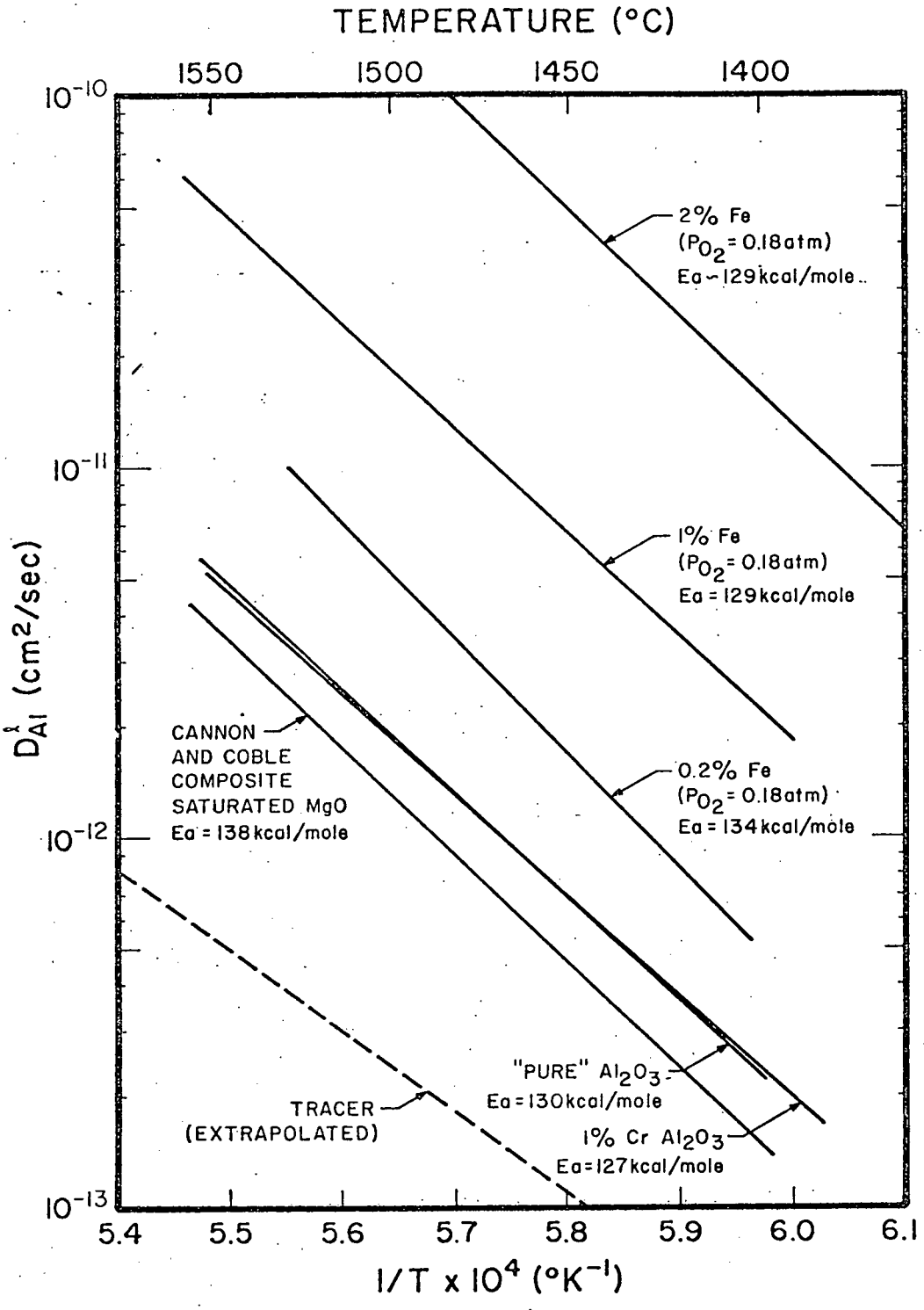

Figure 12 Aluminum Lattice Diffusion Coefficients in Al_2O_3

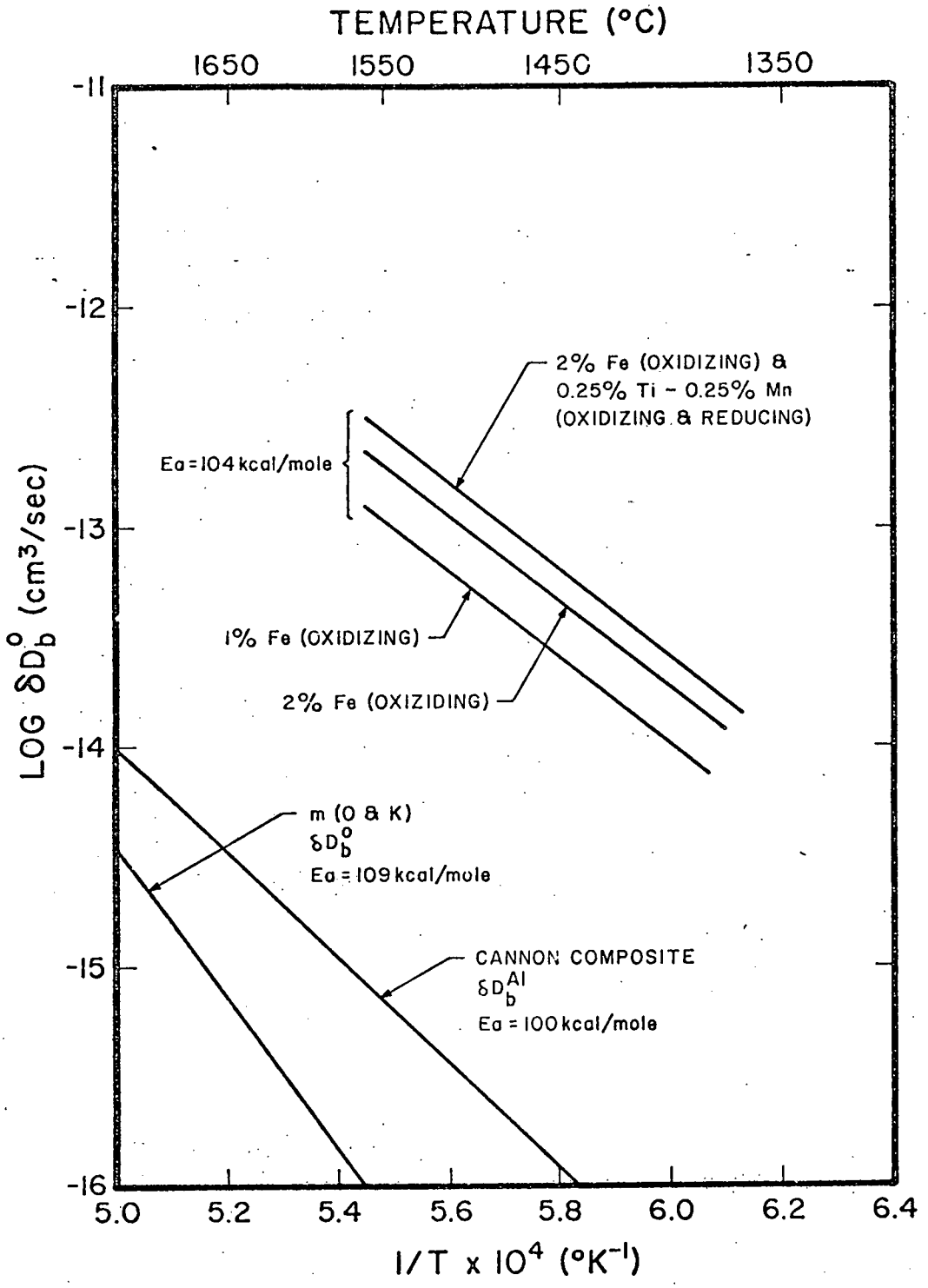

Figure 13 Estimates of Oxygen and Aluminum Grain Boundary Diffusivities in Polycrystalline Al_2O_3

data for $\delta_{Al} D^{b}_{Al}$ (= $8.6 \times 10^{-4} \exp\left(-\frac{100,000}{RT}\right)$ cm^3/sec) which were computed by Cannon and Coble [20] from creep data on fine grained (<10μm) Al_2O_3 (pure and doped with MgO) at low temperatures. Values of $\delta_O D^{b}_{O}$ inferred from abnormal grain growth and oxygen self diffusion in pure Al_2O_3 [21] are also included in Figure 13 for comparison. It is clear from these data that oxygen grain boundary diffusion in doped polycrystalline Al_2O_3 is over three orders of magnitude larger than that in undoped material and over two orders of magnitude larger than aluminum grain boundary diffusion in pure and MgO-doped Al_2O_3. Doping Al_2O_3 with Fe or (Mn - Ti) gives rise to a considerable enhancement in the oxygen grain boundary diffusivity.

2.3.5 Dead-Load Creep of Coarse-Grained Polycrystalline Al_2O_3, Pure and Doped with Chromium

The dead-load creep characteristics of coarse grained (40 - 1200μm) polycrystalline Al_2O_3, pure and doped with chromium are shown in Figure 14. When the grain size exceeded 40 - 70μm the steady state creep rate was no longer reciprocally related to the grain size. In undoped material the creep rate actually increased with increasing grain sizes over 70μm. In chromium-doped Al_2O_3 the creep rate was independent of the grain size for grain sizes over 40 - 60μm. In this grain size independent regime the creep rate decreased with an increase in chromium concentration from 1 to 10% indicating a possible hardening effect.

In the regime of large grain sizes non-viscous creep is much more dominant. The stress exponents at small grain sizes (i.e. $\dot{\varepsilon} \alpha (GS)^{-2}$) increased from 1.03 - 1.30 to 1.4 - 2.9 in the large grain size limit (i.e. $\dot{\varepsilon} \alpha (GS)^{m}$; m = 2 (pure); m = 0 (chromium)). Furthermore, the stress exponents in the large grain size regime were found to be dependent on the temperature. They increased from 1.4 - 1.8 at 1450°C to 2.3 - 2.9 at 1550°C. Due to a change in mechanism the activation energy also changes with temperature. At 1450°C

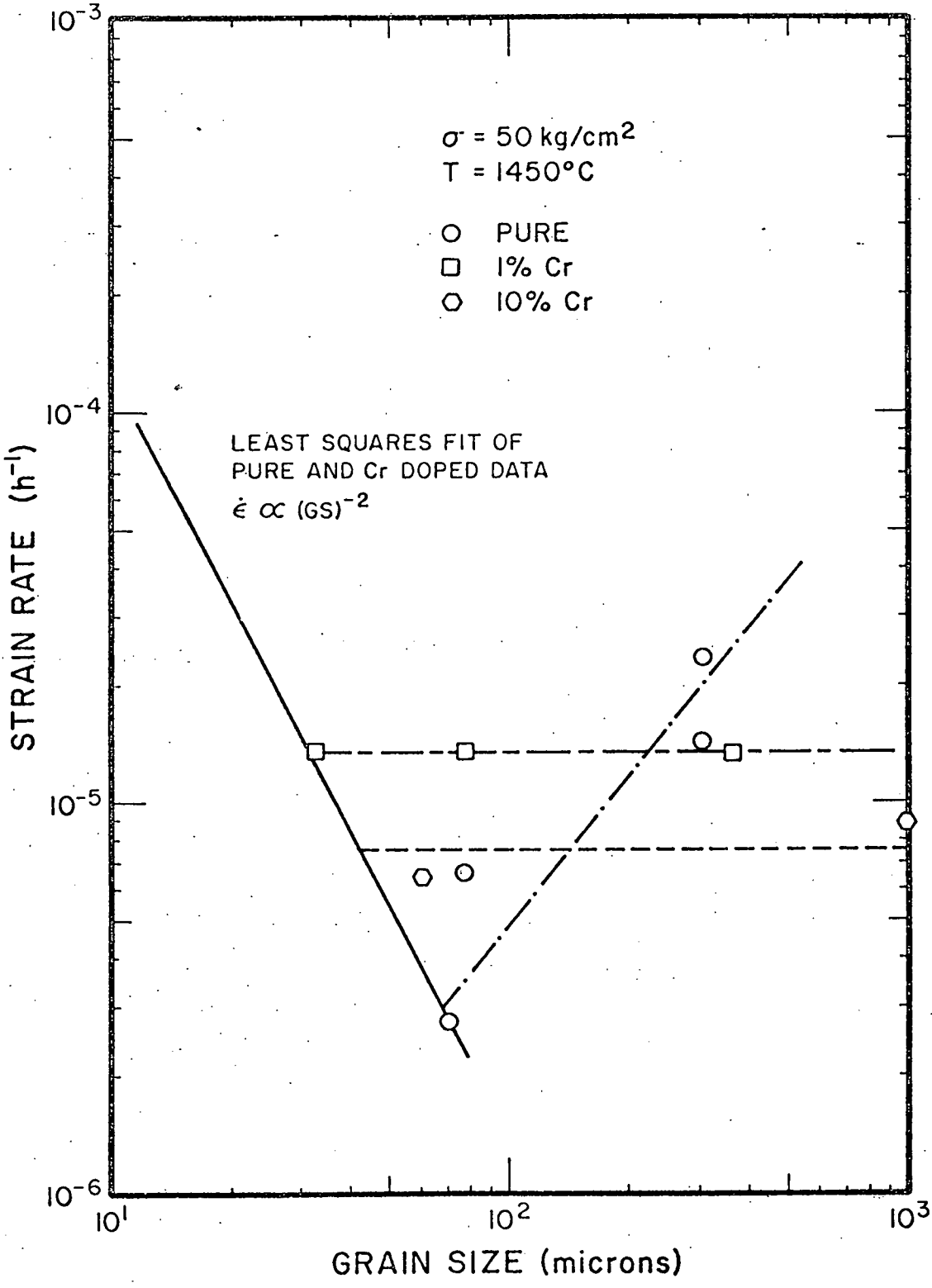

Figure 14 Dead-Load Creep of Coarse-Grained Polycrystalline Al_2O_3, Pure and Doped with Chromium

the activation energy was ∿60 Kcal/mole (undoped Al_2O_3) while at 1575°C, the activation energy increased to approximately 100 Kcal/mole. Power law creep (N ∿ 3-4) has been well documented in previous work on the creep of polycrystalline Al_2O_3 at temperatures over 1600°C. [17] Evidently a transition in mechanism occurs over a range of temperatures (1450-1550°C) from slightly non-viscous behavior (1.4 - 1.8) to definite non-viscous power low creep (N ∿ 3). It is possible that recovery processes such as dislocation climb become important in non-viscous creep at elevated temperatures. These may be responsible for the increase in stress exponents to values around 3 at 1550°C.

2.4 Stress Relaxation Deformation Studies on Polycrystalline Al_2O_3, Pure and Doped with Chromium

In order to achieve high strain rates (∿ $1h^{-1}$) and stresses (∿1000 kg/cm²), which are difficult to achieve in dead-load creep tests on brittle materials because of problems associated with introducing large amounts of strain and premature fracture, a series of stress relaxation tests were conducted on pure and chromium-doped polycrystalline Al_2O_3 to determine (1) the transition between viscous and non-viscous deformation (2) the effect of grain size in the non-viscous deformation regime and (3) if a correlation exists between deformation under conditions of constant load and constant strain (i.e. stress relaxation).

Stress relaxation studies were conducted in four-point bending by a procedure described previously [6]. Viscous creep equations were used to estimate stresses (maximum error is an overestimate of ∿ 30% for N values around 10-12. For N values ∿ 3-4 the error is ∿ 25%). Strain rates were calculated using load point and center of beam deflections. Typically center of beam calculations yielded strain rates 8-10 times slower than those obtained from load-point

calculations. These were found to be in reasonable agreement with strain rates determined under dead-load conditions. All strain rate calculations were made using center point deflections unless noted otherwise.

Typical load relaxation curves for a 44μm undoped specimen tested at 1450°C are shown in Figure 15. Twelve loadings and subsequent load relaxations were completed in this series of experiments. It is clear that a hardening process is taking place with each increment of additional plastic strain. By the eleventh loading, an additional amount of strain resulted in very little additional hardening. It is believed that the structure at this stage represents a steady state configuration for which a direct comparison will exist with data obtained under dead-load conditions. The data in Figure 15 also reveal a transition in behavior from a high stress regime with a large stress exponent (~ 7) to a low stress regime with a much lower stress exponent ($N \sim 1.8 - 1.9$).

When stress relaxation is conducted at the same grain size but at a higher temperature (refer to Figure 16) the stress exponent drops to 3.75 and is characteristic of deformation over four orders of magnitude in strain rate ($1 - 10^{-4}\ h^{-1}$) for a large range of stress (100 - 1000 kg/cm^2). It is possible that recovery processes become important at higher temperatures leading to stress exponents (3 - 4) consistent with processes involving dislocation climb.

Finally, the effect of grain size on non-viscous creep rates at 1450°C is shown in Figure 17. Consistent with experiments under dead-load conditions is the observation of a direct grain size dependence (i.e. creep rates increase as the grain size is increased). Whether or not this grain size dependence would hold at elevated temperatures where dislocation recovery processess are rate controlling remains for further experimentation to check.

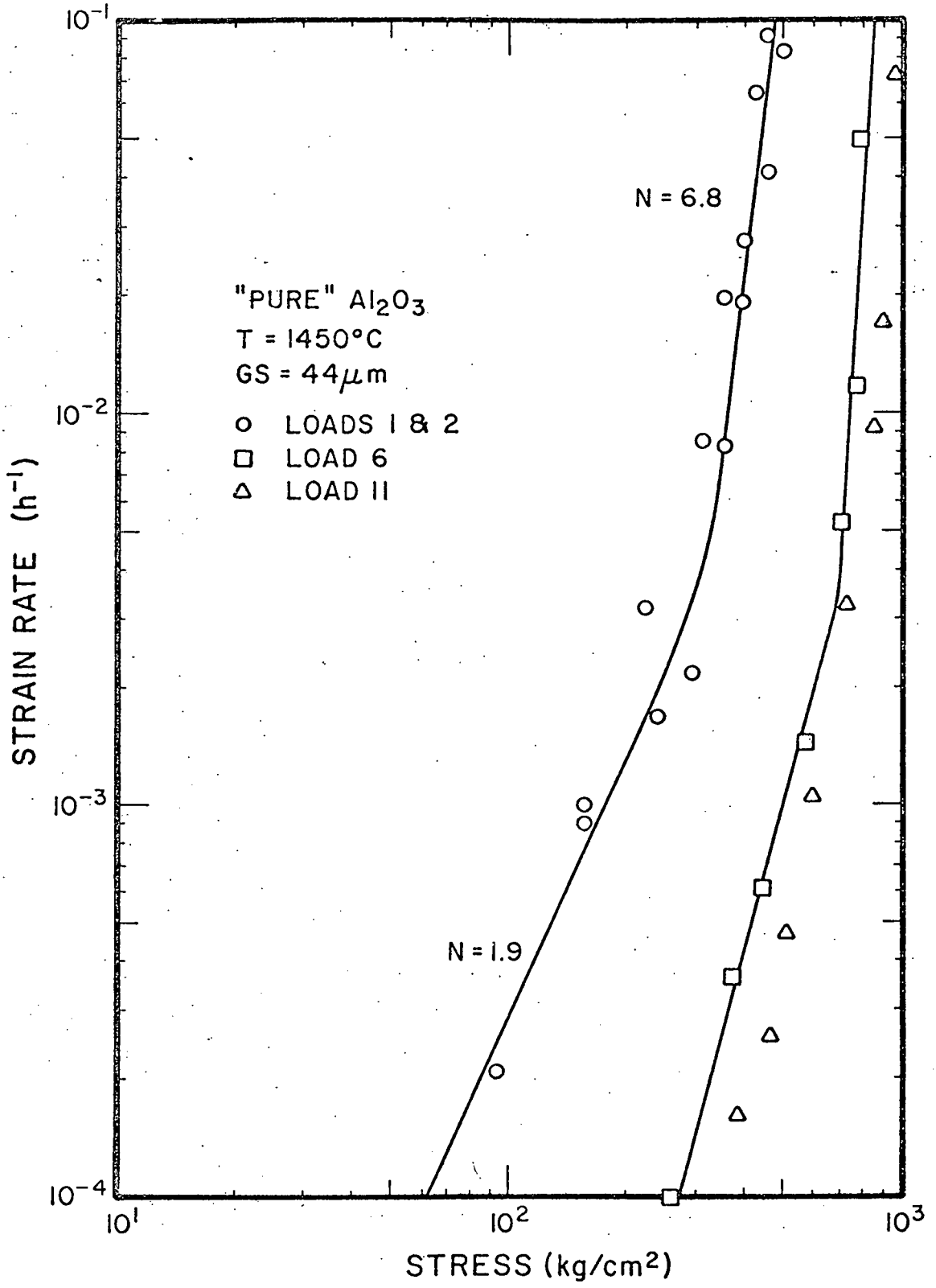

Figure 15 Stress Relaxation at 1450°C in Polycrystalline Al_2O_3

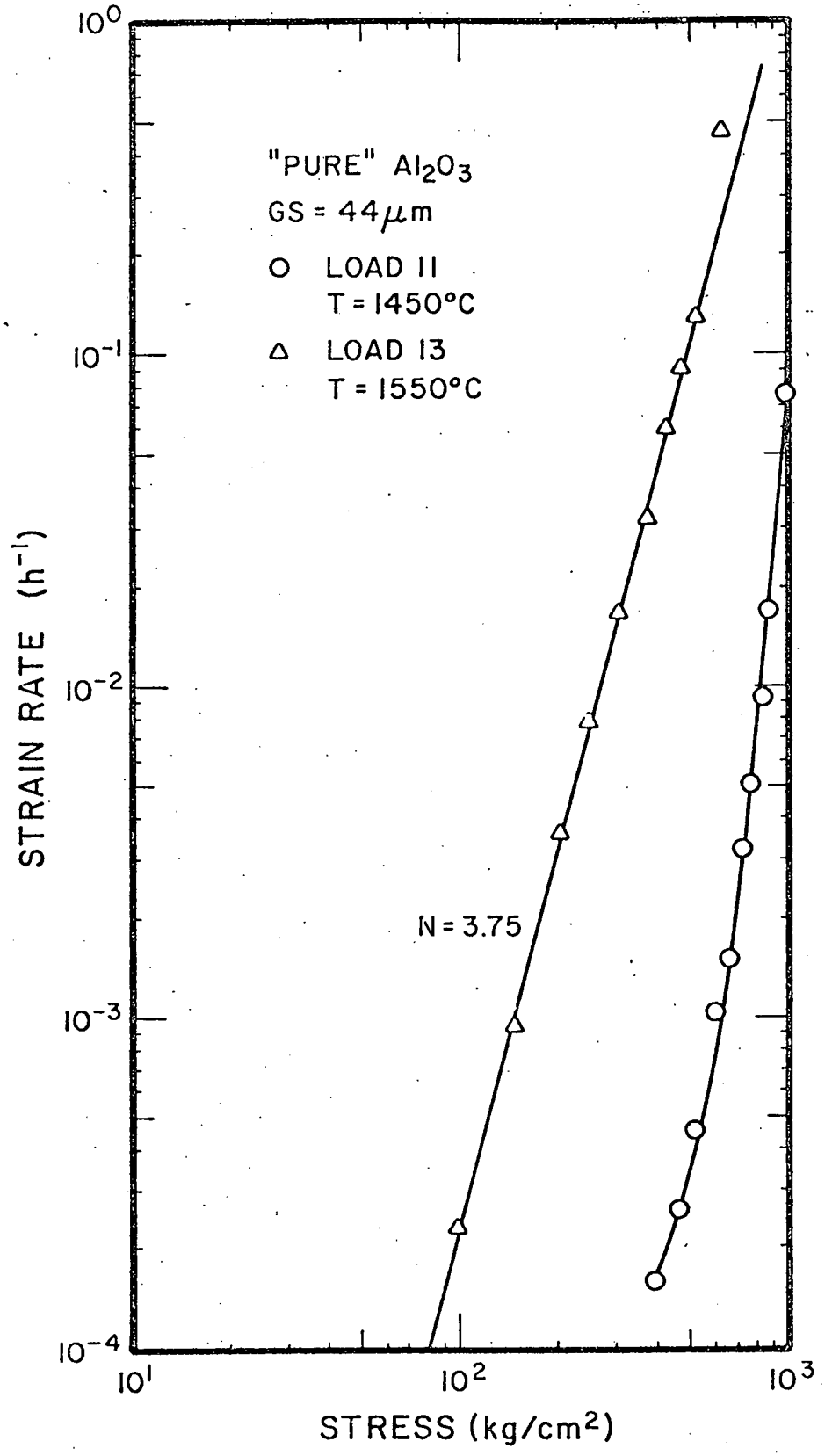

Figure 16 Stress Relaxation at 1450 and 1550°C in Polycrystalline Al_2O_3

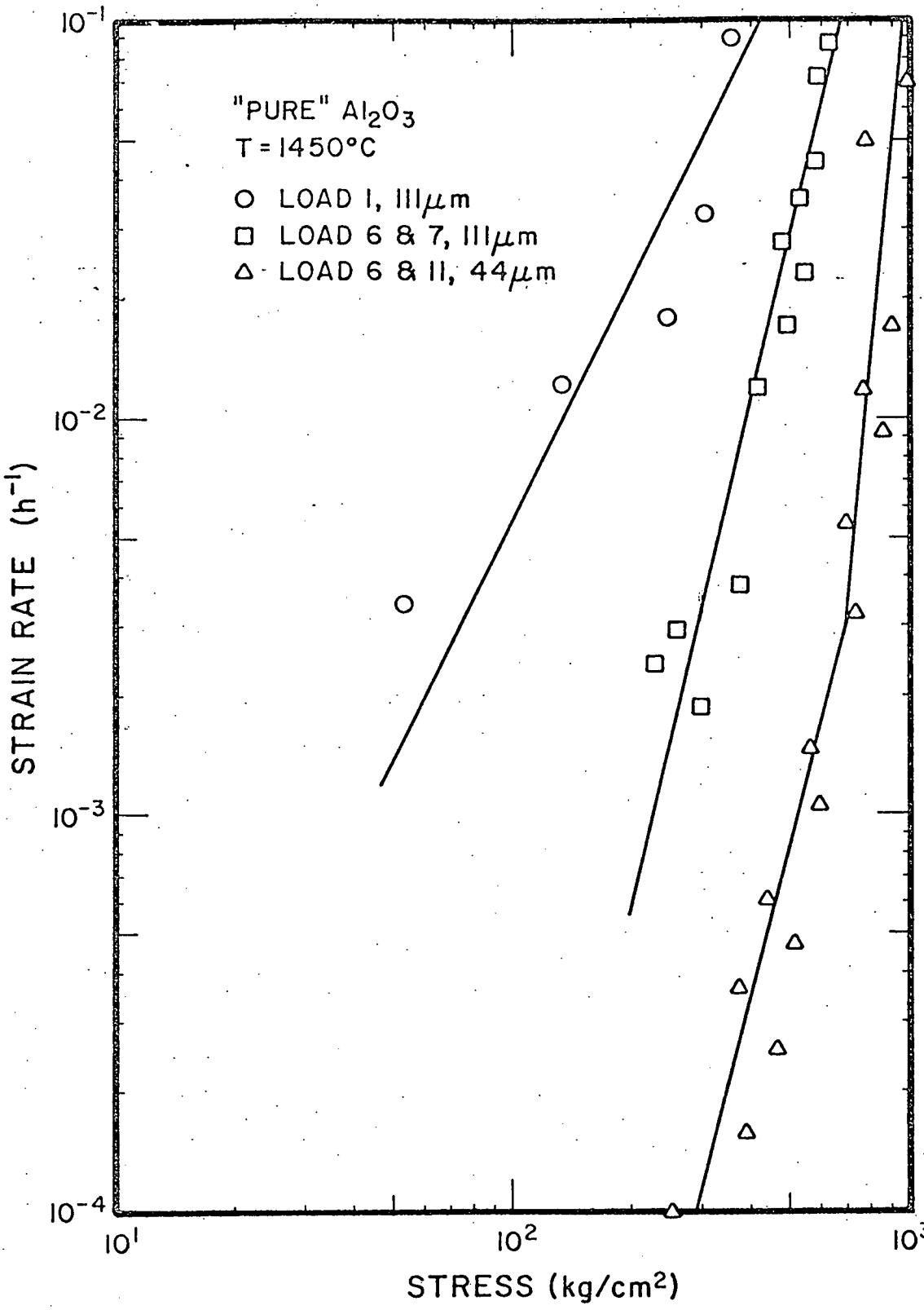

Figure 17 Effect of Grain Size on Stress Relaxation in Polycrystalline Al_2O_3

In Table 5 a comparison is given for stress exponents obtained from dead-load and stress relaxation tests on polycrystalline Al_2O_3. Reasonable agreement exists between the two sets of data. At 1550°C stress exponents in the range of 3 - 4 are common. At a lower temperature (1450°C) stress exponents in the range of 1.4 - 1.9 are characteristic for the deformation of reasonably coarse- grained specimens (44 - 306μm). Slightly non-viscous behavior ($N \gtrsim 1.3$) is dominant in fine-grained material (9 - 72μm) which is tested at intermediate to low stress levels (40 - 500 kg/cm^2).

Typical stress relaxation curves for a chromium-doped (1%) specimen with a grain size of 78μm are shown in Figure 18. Significant hardening was observed in the first eight loadings. Very little additional hardening took place between the tenth and fourteenth loadings. A stress exponent of ~ 7 was determined for stresses over 200 kg/cm^2. A sharp transition to viscous creep was observed at this stress level. After the stress relaxation tests, the same specimen was re-tested under dead-load conditions. The dead-load stress-strain rate behavior in the low stress regime was in remarkably good agreement with the stress relaxation data. This experiment reveals two important features: (1) Dead-load creep data can be matched with data from stress relaxation experiments provided all hardening effects have been removed in the load relaxation tests (i.e. a stable structure exists such that the same $\dot{\varepsilon} - \sigma$ curve is traced on subsequent relaxations). (2) It is possible to detect the transition between nearly viscous behavior and non-viscous creep in the same specimen by conducting stress relaxation tests under conditions of nearly constant strain.

Stress relaxation tests can also be used to study grain size effects on the deformation of chromium doped Al_2O_3. In Figure 19 load relaxation tests at 1450°C are presented for three grain sizes (15, 38, and 78μm). The low stress regime is nearly viscous ($N \sim 1$) and creep rates are reciprocally

Table 5

Strain Rate - Stress Dependencies for the Deformation of Polycrystalline Al_2O_3

A Comparison Between Dead Load and Stress Relaxation Techniques

	Dead Load				Stress Relaxation	
Dopant (cation %)	Stress Exponent (N)	Stress Range (kg/cm^2)	Temperature (°C)	Grain Size (μm)	Stress Exponent (N)	Stress Range (kg/cm^2)
Undoped	1.30 ± 0.15	40-500	1450	9-72	--	--
	--	--	1450	44	1.8 - 1.9	300-700
	--	--	1450	44	~7	700-1000
	1.76	30-300	1450	76	--	--
	--	--	1450	111	~4	200-700
	1.40	40-100	1450	306	--	--
	--	--	1550	44	3.75	80-600
	2.33 - 2.88	40-200	1550	306	--	--
1% Cr	1.03 - 1.30	50-550	1400 - 1500	9-32	--	--
	--	--	1450	15	~1	40-400
	--	--	1450	15-38	9-11	400-1000
	1.43	40-320	1450	77	--	--
	--	--	1450	78	~1	10-100
	--	--	1450	78	~7	100-400
	1.67	40-90	1450	276	--	--

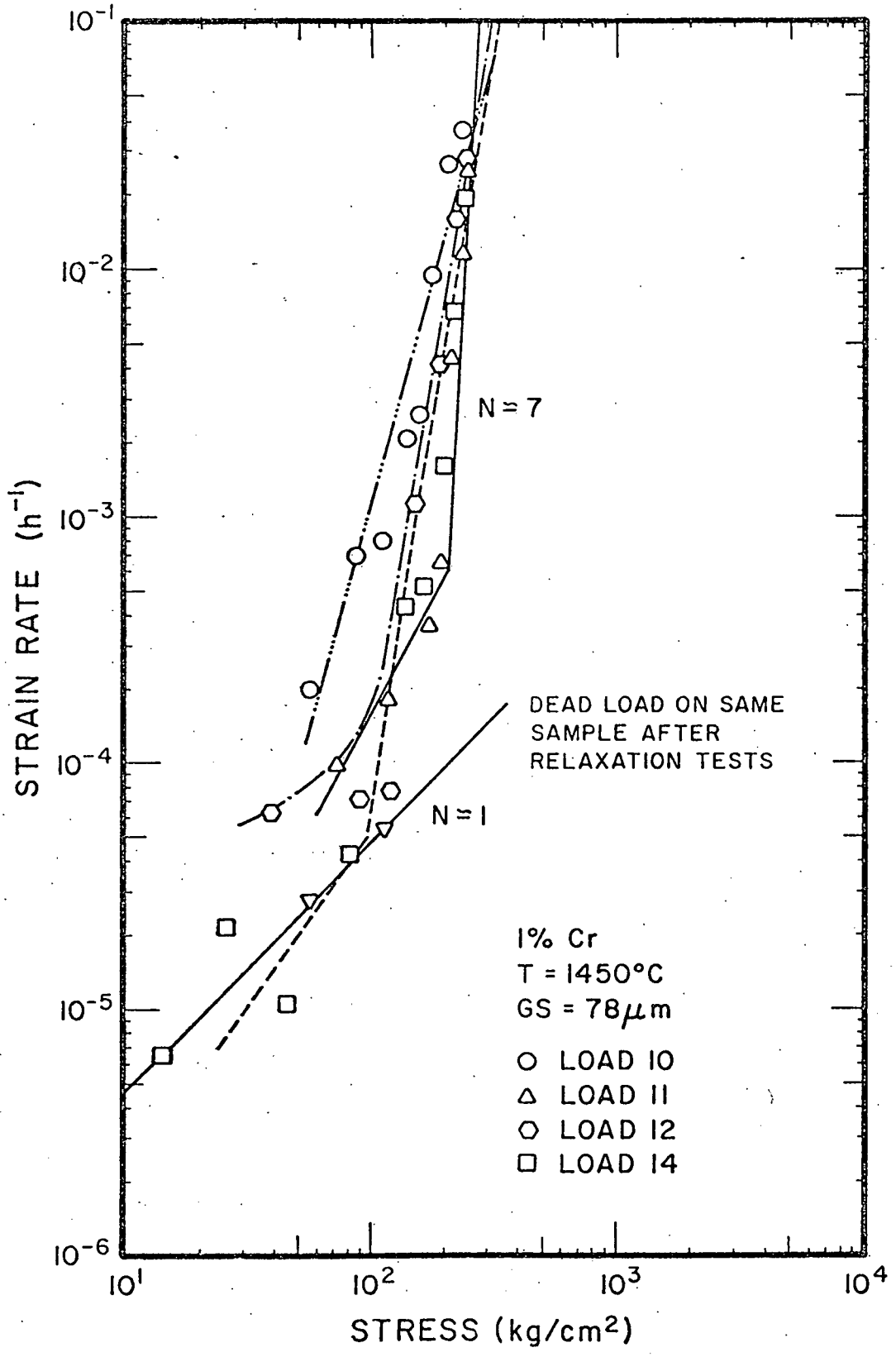

Figure 18 Stress Relaxation at 1450°C in Polycrystalline Al_2O_3 Doped with Chromium

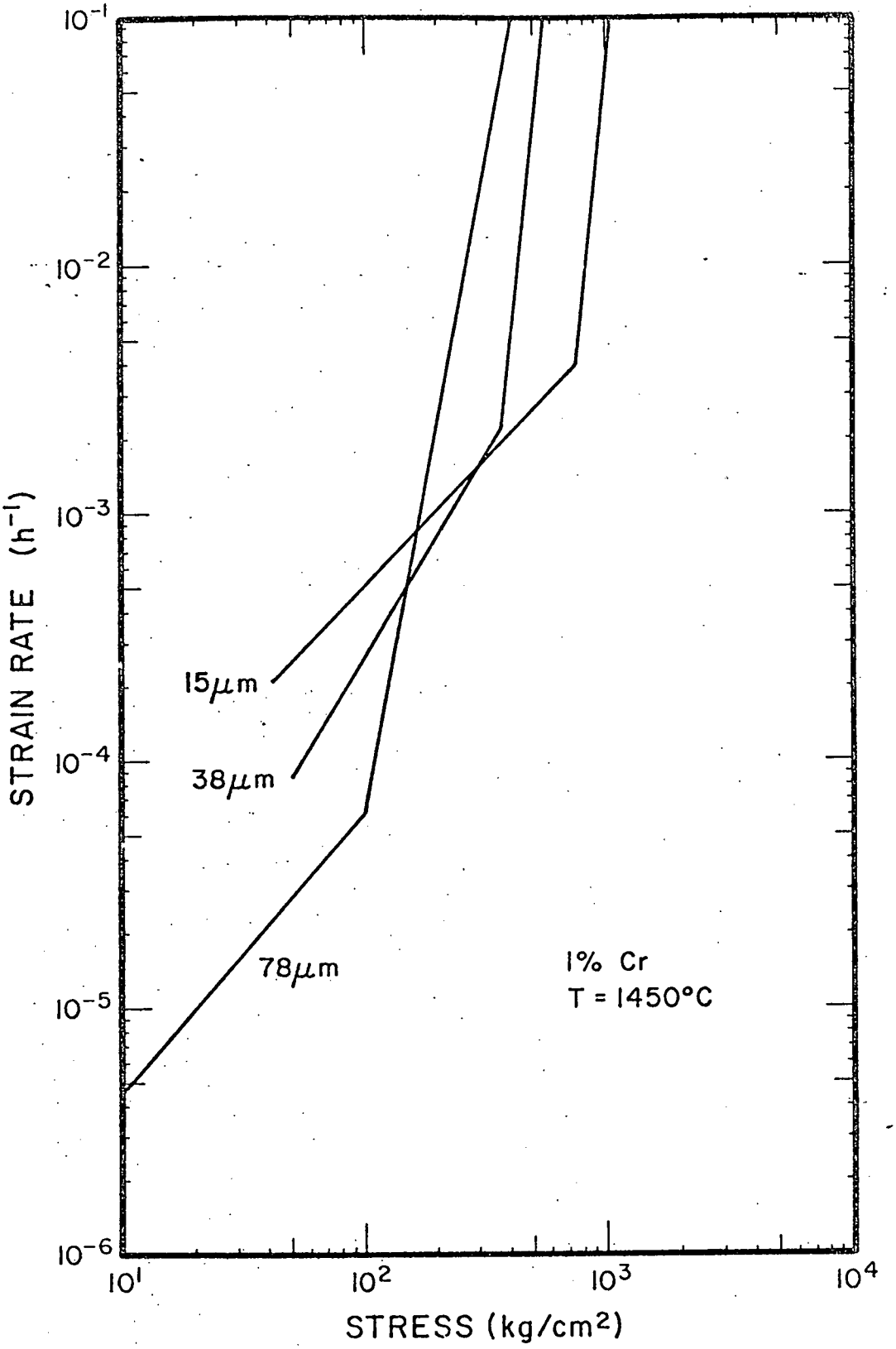

Figure 19 Effect of Grain Size on Stress Relaxation in Polycrystalline Al_2O_3 Doped with Chromium

related to the grain size. The high stress regime (N = 7-11) is definitely non-viscous with creep rates increasing with increases in the grain size.* The transition stress between viscous and non-viscous deformation increases as the grain size decreases as is to be expected.

In Table 5, a comparison is given for stress exponents obtained from dead-load and stress relaxation tests in chromium-doped (1 cation %) polycrystalline Al_2O_3. In the low stress regime (< 400 kg/cm^2) viscous (N = 1) on slightly non-viscous (N $\sim$ 1.3 - 1.7) behavior is dominant. At higher stresses (up to 1000 kg/cm^2), achievable only in load relaxation tests, highly non-viscous (N = 7-11) behavior is observed. Further experiments at higher temperatures are required to see if lower N values (3-4), typical of dislocation climb processes, become dominant. Preliminary indications of this transition are apparent in the dead-load creep data at 1550°C for coarse-grained Al_2O_3 doped with 10% Cr (refer to Table 2).

2.5 Creep Deformation Maps in the MgO and Al_2O_3 Based Systems

Mapping of creep deformation modes for polycrystalline materials (particularly metals) has received renewed interest with the work of Ashby [22] in which lines of constant strain rate (iso-strain rate lines) are computed for variable stresses and temperatures at a fixed grain size. Transitions between viscous and non-viscous creep regimes can be readily identified in maps of this type. Recently Langdon [23] proposed a deformation map in which iso-strain rate lines are computed for variable stresses and grain sizes at a fixed temperature. This map is particularly useful for material in which diffusional creep modes are important since they are very grain size dependent. Another map which is useful for diffusional creep regimes consists of iso-strain rate lines computed with variable temperatures and grain sizes at a fixed level of stress.

*This is an apparent contradiction with dead-load creep tests at small stresses ($\sim$ 40 μm) in which no grain size effects were observed.

Sufficient creep data now exist for polycrystalline MgO and Al_2O_3, pure and doped with iron, that it is worthwhile to construct creep deformation maps to illustrate graphically the important deformation mechanisms which operate in these systems and the range of variables over which they are dominant. In Table 6, a summary is given of the six deformation maps which will be presented in this report. All of the deformation maps summarized in Table 6 were constructed from experimental data obtained during the course of this contract. Some data, particularly for fine-grained Al_2O_3, were taken from the recent work of Cannon and Coble [20]. A summary of the input data will be given for each deformation map. In the diffusional creep regimes equations [7] and [8] will be used for Nabarro-Herring and Coble creep regimes, respectively.

$$\dot{\varepsilon} = \frac{14\Omega_v \sigma D^{\ell}}{kT(GS)^2} \qquad [7]$$

$$\dot{\varepsilon} = \frac{44\Omega_v \sigma \delta D^{b}}{kT(GS)^3} \qquad [8]$$

For MgO and Al_2O_3 based systems, two boundary diffusion processes will be important: cation and anion grain boundary diffusion. In some situations, diffusional creep will be a mixture of cation lattice and anion grain boundary diffusion. In this case, the following equation will be employed to calculate strain rates*.

$$\dot{\varepsilon} = \frac{44\Omega_v \sigma}{\pi\, kT(GS)^2} \; D_{complex} \qquad [9]$$

$$D_{complex} = \frac{D^{\ell}/\alpha}{1 + (\beta/\alpha)(\frac{GS}{\pi})\frac{D^{\ell}}{\delta D^{b}}}$$

In a few situations some deformation regimes were determined from estimates of mass transport parameters and activation energies.

---

*For MgO $\alpha = \beta = 1$

For Al_2O_3 $\alpha = 2$ and $\beta = 3$

Table 6

Creep Deformation Maps for Polycrystalline MgO and Al_2O_3

Material	Impurity and Concentration (cation %)	Variables	Fixed Variable
MgO	Undoped	σ, (GS)	T
MgO	Fe (0.53)	σ, (GS)	T
MgO	Fe (2.65)	T, (GS)	σ
Al_2O_3	Undoped	σ, (GS)	T
Al_2O_3	Fe (1.0)	T, (GS)	σ
Al_2O_3	Fe (2.0)	T, (GS)	σ

Finally, it is noted that transitions between different deformation regimes are indicated on the creep maps by single lines. It is to be emphasized that these lines represent situations where the creep rates of the two processes in question are equal. It must be remembered that in the vicinity of the boundaries deformation modes are mixed. In particular, mixed modes of deformation may exist in diffusional creep regimes over several orders of magnitude in strain rate.

2.5.1 Polycrystalline MgO, Pure and Doped with Iron

In Figure 20 the creep map for undoped magnesium oxide is presented at 1350°C. The input data are summarized in Table 7. The diffusional creep data were obtained from experiments on hot-pressed material in which LiF was used as a pressing aid. The diffusion coefficients (D^{ℓ}_{Mg} and $\delta_{Mg}D^{b}_{Mg}$) may be overestimated by up to factor of 3 and, hence, the diffusional creep regimes may actually lie at somewhat lower stresses and grain sizes than those indicated on the present map. Even though two separate diffusional modes are indicated, a large portion of this regime is mixed in character [6].

The non-viscous regime was determined from dead-load creep data at 1500°C taken on a large-grained specimen (218μm) and corrected to 1350°C using an activation energy of 80 Kcal/mole. Both dead-load and stress relaxation experiments were in agreement in the non-viscous regime for stresses up to ~700 kg/cm^2. The insensitivity of the non-viscous process to grain size is to be noted.

The deformation map clearly indicates that diffusional regimes are dominant at low stresses and small grain sizes. As the grain size increases the transition to non-viscous (dislocation) creep occurs at lower stresses. Ambipolar diffusion theory predicts that diffusional creep will be rate-limited by magnesium grain boundary diffusion at small grain sizes (< 10-20 μm) and by

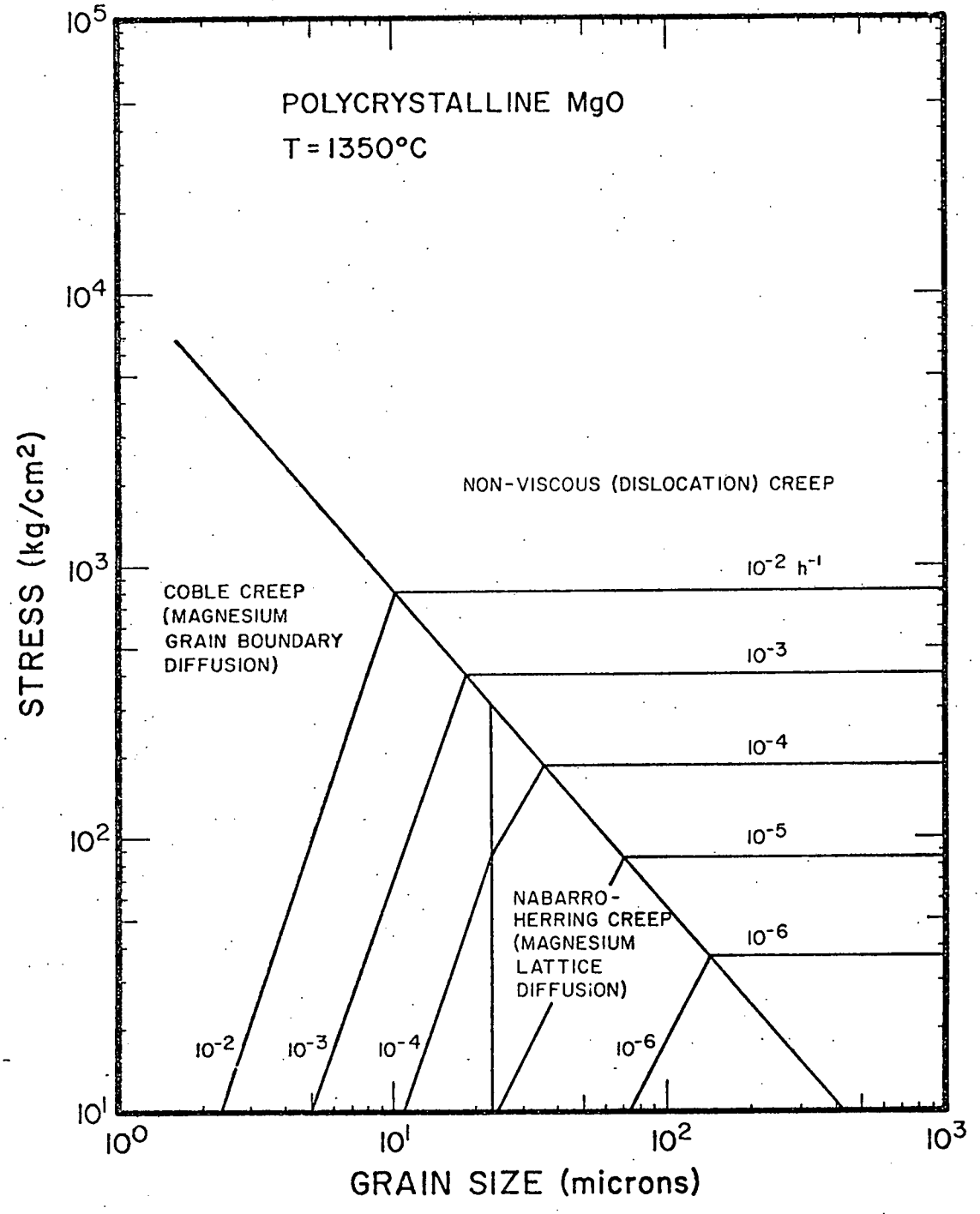

Figure 20 Deformation Map for Polycrystalline MgO at 1350°C

Table 7

Input Data for the Creep Deformation Map
on Undoped MgO at 1350°C

Non-Viscous Dislocation Regime

$$\dot{\varepsilon}(h^{-1}) = 1.30\ \sigma^{3.0}\ (GS)^{0}\ \exp\left(-\frac{80{,}000}{RT}\right)$$

Nabarro-Herring (Magnesium Lattice Diffusion)

$\Omega_v = 1.86 \times 10^{-23}$ cm^3

$D_{Mg}^{\ell} = 1.53 \times 10^{-12}$ cm^2/sec in Equation [7]

Coble (Magnesium Grain Boundary Diffusion)

$\delta_{Mg} D_{Mg}^{b} = 1.19 \times 10^{-15}$ cm^3/sec in Equation [8]

magnesium lattice diffusion at larger grain sizes (up to ∿100μm) providing oxygen grain boundary diffusion is very fast. Most of the previous deformation maps [23] in MgO have been constructed assuming that oxygen lattice diffusion and/or grain boundary diffusion are rate controlling. Actually oxygen grain boundary diffusion will be rate limiting only at very large grain sizes (> 200μm) and very small stresses (a regime which is difficult to detect experimentally). Creep maps which are constructed from constitutive equations based on a single diffusing species (e.g. metals) will give erroneous conclusions regarding the deformation of a polycrystalline ionic compound which involves the coupled diffusion of anions and cations [3].

In Figure 21 the effect of doping polycrystalline MgO with iron (0.53 cation %) is shown in another creep deformation map. The input data for this map are summarized in Table 8. Estimates of $\delta_{Mg}D^{b}_{Mg}$ and $\delta_{O}D^{b}_{O}$ were taken from data at the 0.05 and 2.65 cation % dopant levels, respectively. Non-viscous creep was measured at larger grain sizes (∿ 300μm) at 1500°C and corrected to 1350°C using an activation energy of 71 Kcal/mole.

The effect of iron doping is clearly illustrated by an expansion of the diffusional creep fields to higher stresses and grain sizes as compared to the undoped oxide (Figure 20). The non-viscous creep rates are essentially identical to those of the undoped specimens.

Three diffusional mechanisms are indicated in the viscous creep regime: (1) magnesium grain boundary diffusion at grain sizes below about 14μm , (2) magnesium lattice diffusion for intermediate grain sizes (14-200μm) and (3) oxygen grain boundary diffusion at very large grain sizes (> 200μm). All of the experimental data to data have fallen in the intermediate grain size range (15-100μm) which falls inside the Nabarro-Herring field. Experiments at smaller grain sizes are complicated because of problems associated with fabrication and excessive grain growth. At larger grain sizes creep rates become undetectable

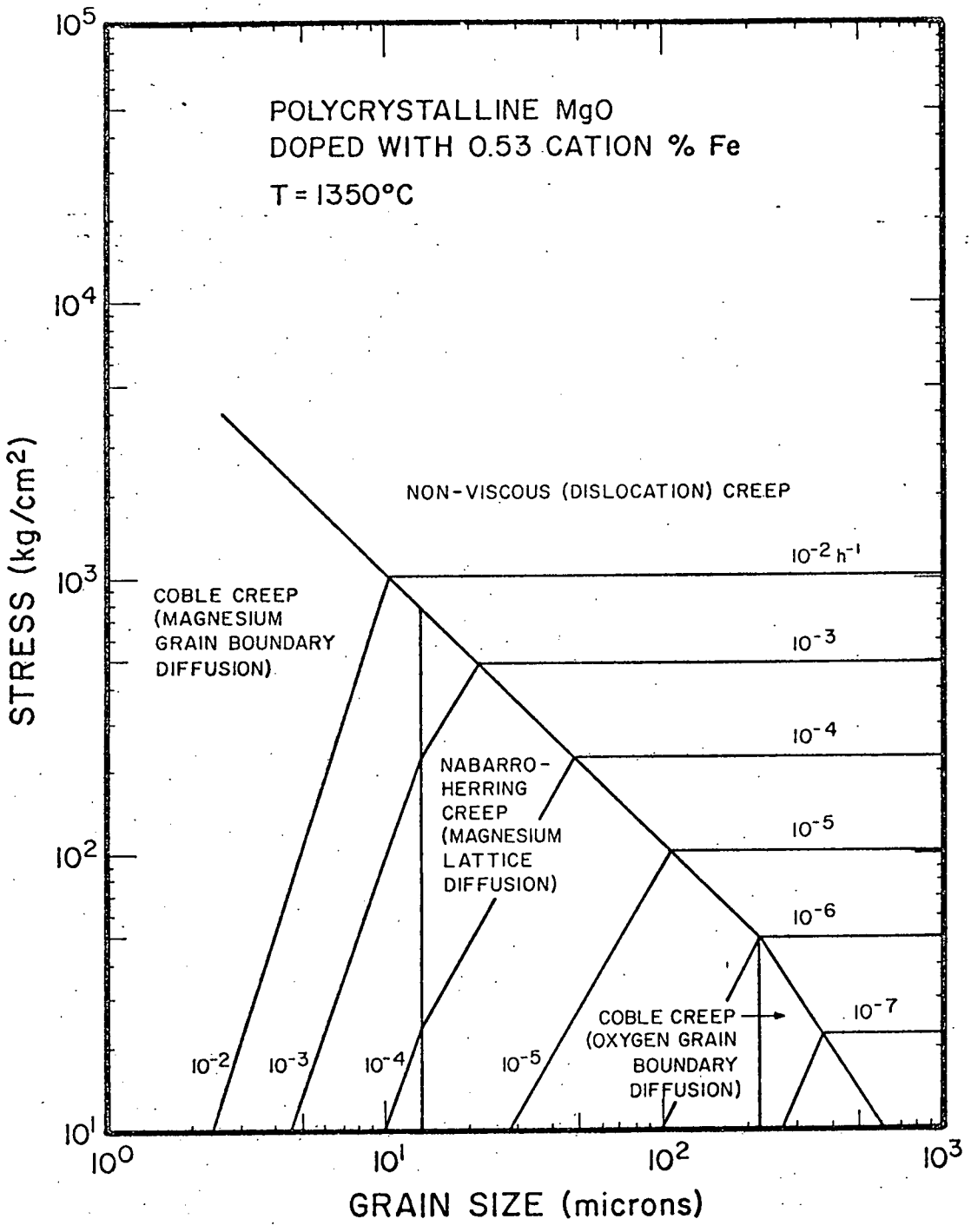

Figure 21 Deformation Map at 1350°C for Polycrystalline MgO Doped with 0.53 cation % Iron

Fig 21

Table 8

Input Data for the Creep Deformation Map at 1350°C
for MgO Doped with 0.53 Cation % Fe

Non-Viscous Dislocation Regime

$$\dot{\varepsilon}(h^{-1}) = 3.12 \times 10^{-2}\ \sigma^{3.0}\ (GS)^{0}\ \exp -\left(\frac{71{,}000}{RT}\right)$$

Nabarro-Herring (Magnesium Lattice Diffusion)

$D_{Mg}^{\ell'} = 2.3 \times 10^{-12}$ cm^2/sec in Equation [7]

Coble (Magnesium Grain Boundary Diffusion)

$\delta_{Mg} D_{Mg}^{b} = 7.3 \times 10^{-16}$ cm^3/sec in Equation [8]

Coble (Oxygen Grain Boundary Diffusion)

$\delta_{O} D_{O}^{b} = 1.6 \times 10^{-14}$ cm^3/sec in Equation [8]

($\leq 10^{-6}$ h^{-1}) at the stress levels required for diffusional creep (< 50-100 kg/cm^2).

To illustrate the effect of temperature on diffusional creep in iron-doped polycrystalline MgO, a creep deformation map (Figure 22) was constructed for the 2.65% dopant level at a constant stress (100 kg/cm^2) with temperature and grain size as the primary variables. The input data for the map in Figure 22 are summarized in Table 9. Several interesting features are apparent in this new type of deformation map. Two regimes of Coble creep are present, one at low temperatures and small grain sizes (magnesium grain boundary diffusion) and the other at high temperatures and large grain sizes (oxygen grain boundary diffusion). This behavior is in marked contrast to that encountered in metals (single diffusing species) for which Coble creep is predicted only at low temperatures and for small grain sizes. Since the activation energy for grain boundary diffusion is less than that for lattice diffusion, the transition grain sizes between consecutive Coble and Nabarro-Herring regimes decrease as the temperature is increased. Much of the deformation is mixed in character (i.e. $D_{Mg}^{\ell} (\frac{GS}{\pi}) \approx \delta_O D_O^b$) for the variables which are achievable experimentally (i.e. 10μm $\leq$ GS $\leq$ 100μm, 5×10^{-6} $h^{-1} \leq \dot{\varepsilon} \leq 5 \times 10^{-3}$ h^{-1}) in the dead-load creep test. The regime of Coble creep controlled by magnesium grain boundary diffusion may exist at lower temperatures and grain sizes since values of $\delta_{Mg} D_{Mg}^b$ have probably been overestimated.

Finally, the non-viscous regime was assumed to be identical to that measured at the 0.53% dopant level in the large grain size limit (100-500μm). Non-viscous creep in polycrystalline MgO is both independent of grain size and iron-doping. Of course, as the stress is increased, the non-viscous modes would become dominant at lower temperatures and smaller grain sizes.

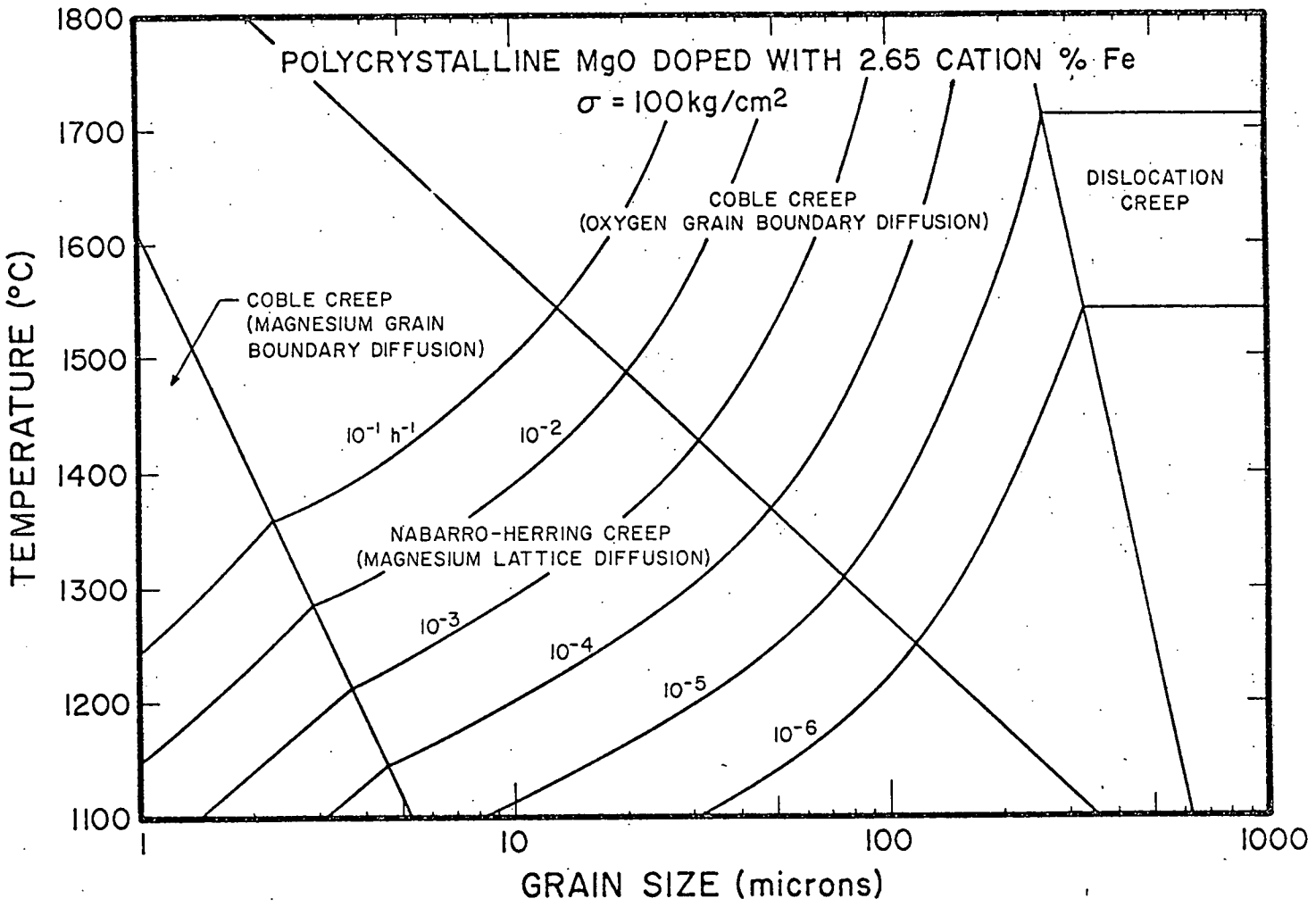

Figure 22 Deformation Map at Constant Stress (100 kg/cm^2) for Polycrystalline MgO Doped with 2.65 cation % Iron

Table 9

Input Data for the Creep Deformation Map at
100 kg/cm^2 for MgO Doped with 2.65% Iron

Non-Viscous Dislocation Regime

$$\dot{\varepsilon}(h^{-1}) = 3.12 \times 10^{-2}\ \sigma^{3.0}\ (GS)^{0}\ \exp\left(-\frac{71{,}000}{RT}\right)$$

Nabarro-Herring (Magnesium Lattice Diffusion) and Coble (Oxygen Grain Boundary Diffusion)

Equation [9] was used with the following transport parameters:

$$D_{Mg}^{\ell} = 5.06 \times 10^{4}\ \exp\left(-\frac{117{,}000}{RT}\right)\ cm^2/sec$$

$$\delta_O D_O^b = 4.91 \times 10^{-8}\ \exp\left(-\frac{55{,}800}{RT}\right)\ cm^3/sec^*$$

*Activation energy is an upper bound estimate

Coble (Magnesium Grain Boundary Diffusion)

$$\delta_{Mg} D_{Mg}^{b} = 3.68 \times 10^{-9} \exp\left(-\frac{55{,}800}{RT}\right)\ cm^3/sec$$

Estimated value at 1350°C and activation energy for use in Equation [8]

2.5.2 Polycrystalline Al_2O_3, Pure and Doped with Iron

A creep map at 1450°C for undoped polycrystalline Al_2O_3 is shown in Figure 23. The input data are summarized in Table 10. The Coble creep regime at small grain sizes was constructed from the value of $\delta_{Al} D_{Al}^{b}$ reported by Cannon and Coble [20] to be representative of a composite data analysis for the creep of fine-grained (1-15μm), pure and MgO-doped Al_2O_3. Grain sizes between approximabely 6 and 15μm are predicted for the transition between Coble creep controlled by aluminum grain boundary diffusion and Nabarro-Herring creep controlled by aluminum lattice diffusion. These may be on the high side since Nabarro-Herring creep was observed in this study at grain sizes down to 6μm at 50 kg/cm^2).

All of the measurements taken in this contract fall primarily in the Nabarro-Herring range (6μm < GS < 70μm). Due to the slightly non-viscous nature of the Nabarro-Herring creep regime, the transition between Coble and N-H creep shifts to slightly smaller grain sizes as the stress increases.

Non-viscous creep modes were determined both by stress relaxation and dead-load creep techniques. High stress exponents (1.76 - 4.3) and positive grain size exponents have been incorporated into the deformation map.

The non-viscous data should be considered only preliminary at this stage. However, they do reveal an interesting possibility regarding the selection of a creep resistant alumina. Because of the shift in grain size dependence, a narrower range of grain size exist which give maximum creep resistance at the highest possible stress. For example, at strain rates around 10^{-4} to 10^{-5} h^{-1} grain sizes in the 50 to 100μm range are required to sustain stress between 100 and 300 kg/cm^2. Further experiments are needed at higher temperatures where stress exponents are around 3 to see if the positive grain size dependence remains or if the creep rate becomes independent if the grain size as was the case with MgO.

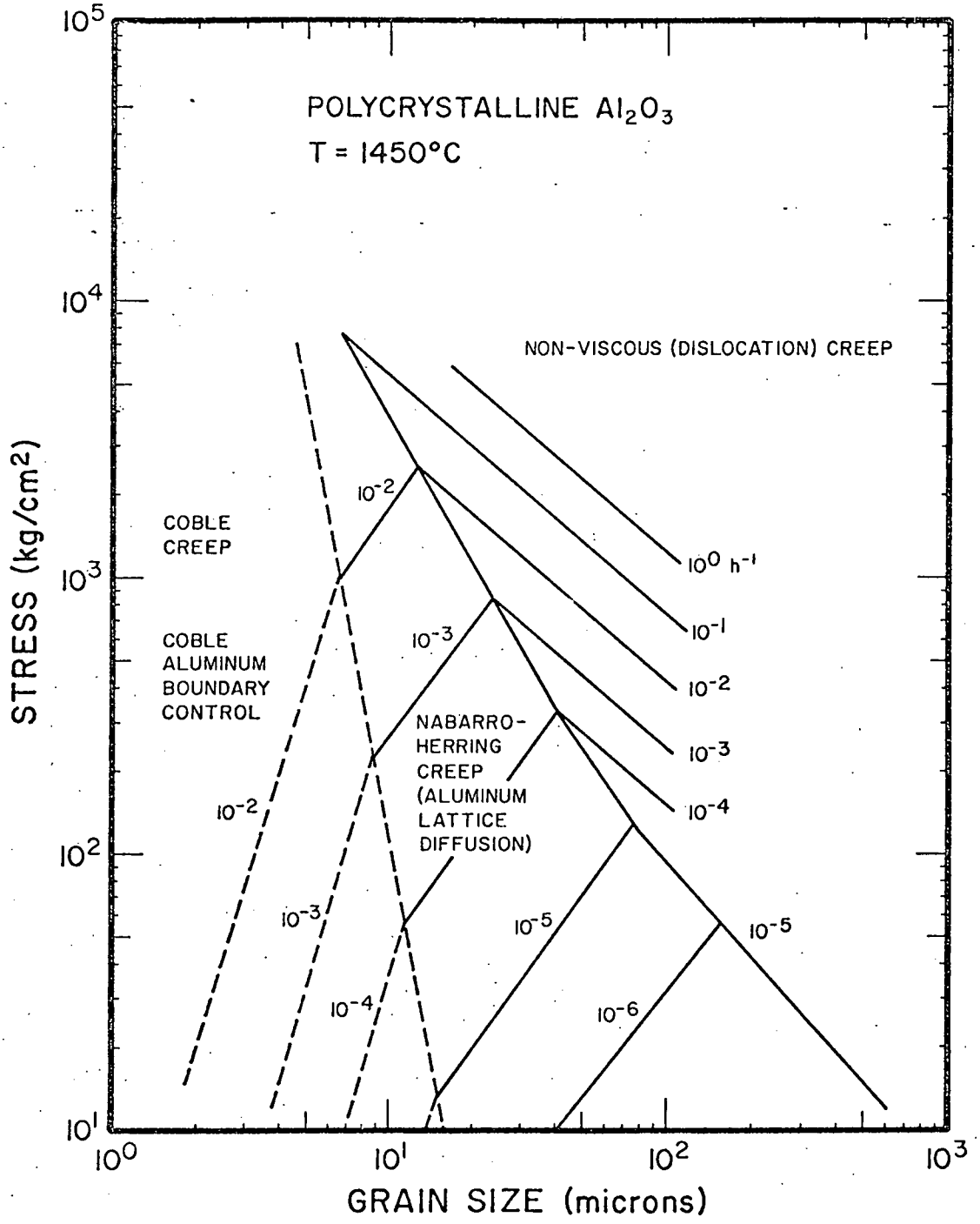

Figure 23 Deformation Map for Polycrystalline Al_2O_3 at 1450°C

Fig 23

Table 10

Input Data for the Creep Deformation Map

on Undoped Al_2O_3 at 1450°C

Coble (Aluminum Grain Boundary Diffusion)

$\Omega_v = 4.27 \times 10^{-23}$ cm^3 and

$\delta_{Al} D_{Al}^b = 8.6 \times 10^{-4} \exp\left(-\frac{100{,}000}{RT}\right)$ cm^3/sec in Equation [8]

Nabarro-Herring (Aluminum Lattice Diffusion)

$\dot{\varepsilon}(h^{-1}) = 4.36 \times 10^{-5} \sigma^{1.3} (GS)^{-1.8}$

Non-Viscous Modes (Small Grain Sizes)

From stress relaxation data

$\dot{\varepsilon}(h^{-1}) = 2.1 \times 10^{-21} \sigma^{4.3} (GS)^{3.7}$

Non-Viscous Modes (Large Grain Sizes)

From dead-load data

$\dot{\varepsilon}(h^{-1}) = 3.27 \times 10^{-13} \sigma^{1.76} (GS)^{2.0}$

The effect of doping polycrystalline Al_2O_3 with a variable valent (Fe^{2+} - Fe^{3+}) impurity is shown for two dopant levels (1 and 2 cation %) in Figures 24 and 25. The input data for these two deformation maps are summarized in Table 11.

The Coble creep regime at low temperatures and small grain sizes was based on Cannon and Coble's [20] evaluation of $\delta_{Al}D^{b}_{Al}$ for undoped and MgO-doped Al_2O_3. Most of the observed creep behavior was a mixture of two mechanisms: (1) Nabarro-Herring creep controlled by aluminum lattice diffusion and (2) Coble creep controlled by oxygen grain boundary diffusion.

At the 1% dopant level and a fixed low stress of 50 kg/cm^2 three diffusional creep mechanisms can operate. For small grain sizes (< 10μm) and low temperatures (< 1300°C) Coble creep, which is rate-limited by aluminum boundary diffusion, is predicted to be dominant. At higher temperatures and larger grain sizes, an extremely broad range exists where both aluminum lattice and oxygen grain boundary diffusion are coupled.

As cation lattice diffusion is enhanced by doping with divalent iron, oxygen grain boundary diffusion gradually becomes the rate limiting step. This effect can be seen by referring to the map for the 2% dopant (Figure 25). Aluminum lattice diffusion has increased to the point that Coble creep controlled by aluminum grain boundary diffusion is almost non-existent. Furthermore, the influence of oxygen grain boundary diffusion as the rate-determining process has shifted to lower temperatures and smaller grain sizes. Figures 24 and 25 represent deformation maps for creep tests in an oxidizing air atmosphere. When creep tests at the 2% dopant were conducted in a reducing environment ($P_{O_2} \sim 10^{-7}$ atm), the deformation process was completely dominated by oxygen grain boundary diffusion at 1450°C for grain sizes between 18 and 83μm. Thus the transition between Nabarro-Herring and Coble creep had shifted to even lower temperatures and smaller grain sizes.

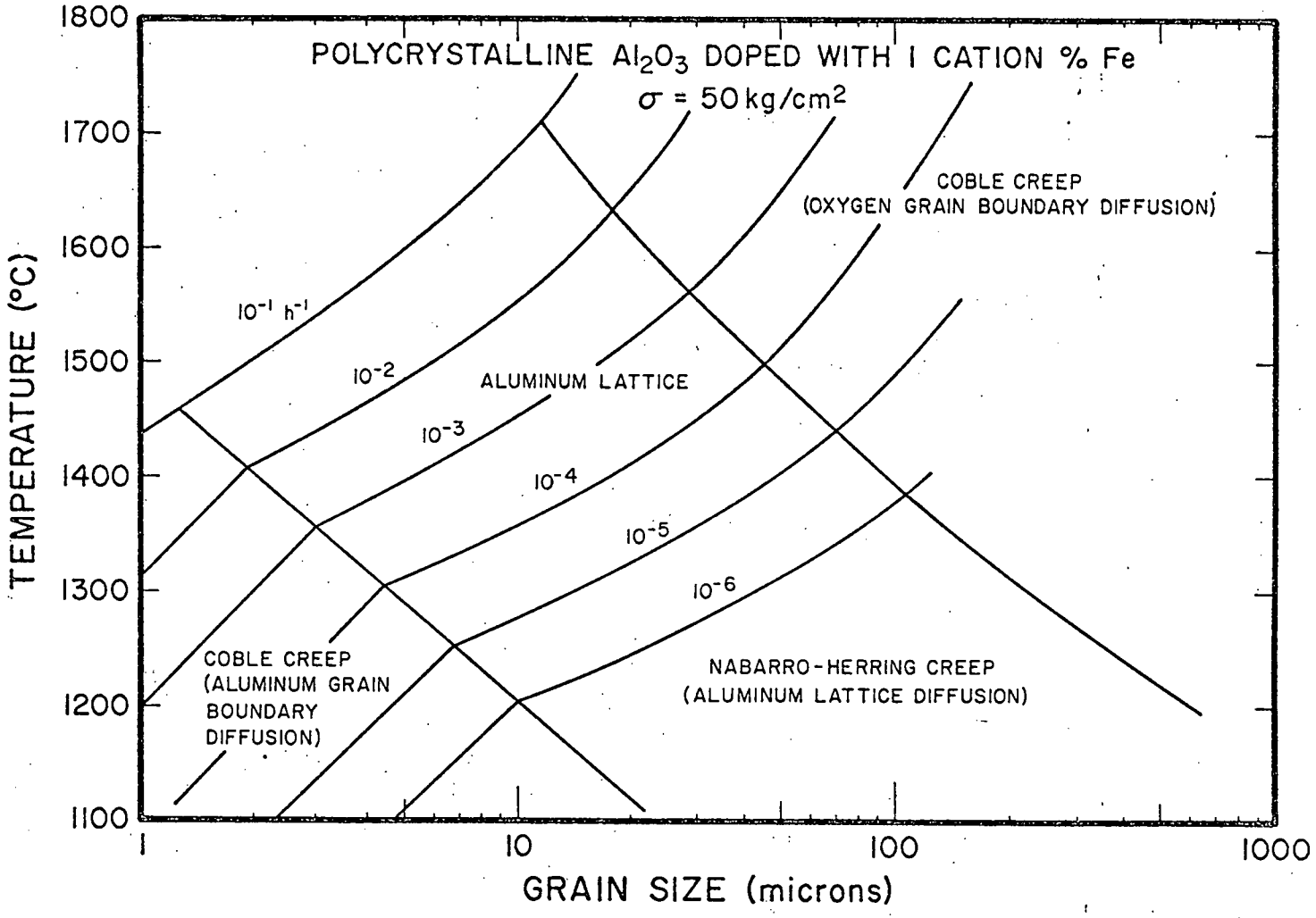

Figure 24 Deformation Map at Constant Stress (50 kg/cm^2) for Polycrystalline Al_2O_3 Doped with 1 Cation % Iron

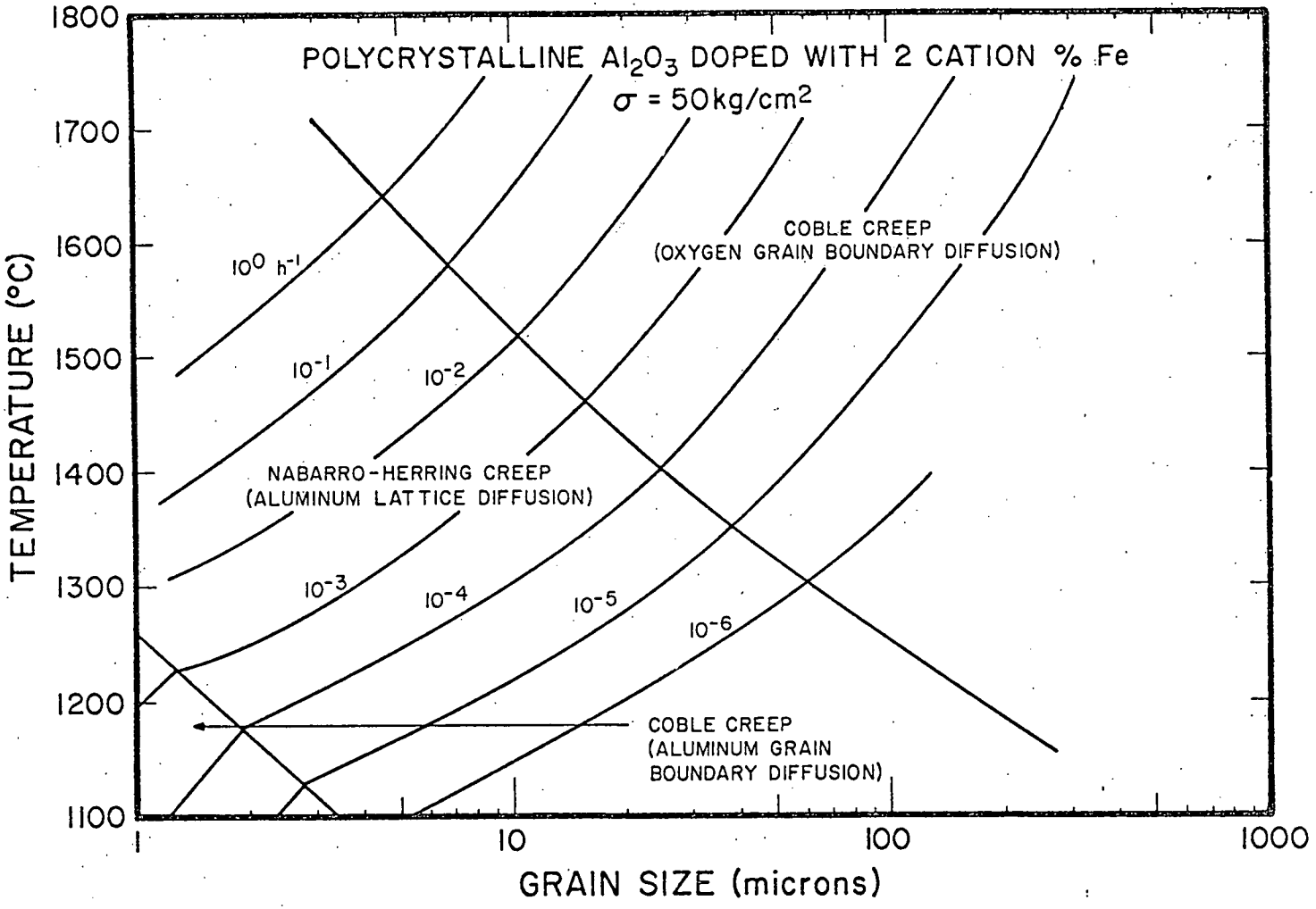

Figure 25 Deformation Map at Constant Stress (50 kg/cm^2) for Polycrystalline Al_2O_3 Doped with 2 Cation % Iron

Table 11

Input Data for the Creep Deformation Maps in Iron-Doped Polycrystalline Al_2O_3

Coble (Aluminum Grain Boundary Diffusion)

$$\delta_{Al} D^{b}_{Al} = 8.6 \times 10^{-4} \exp\left(-\frac{100{,}000}{RT}\right) \text{ cm}^3/\text{sec} \text{ in Equation [8]}$$

Nabarro-Herring (Aluminum Lattice Diffusion) and Coble (Aluminum Grain Boundary Diffusion)

For use in Equation [9]

$$D^{\ell}_{Al} \text{ (1\% Fe)} = 7.15 \times 10^{7} \exp\left(-\frac{150{,}000}{RT}\right) \text{ cm}^2/\text{sec}$$

$$\delta_{Al} D^{b}_{Al} \text{ (1\% Fe)} = 4.38 \times 10^{-1} \exp\left(-\frac{105{,}000}{RT}\right) \text{ cm}^3/\text{sec}$$

$$D^{\ell}_{Al} \text{ (2\% Fe)} = 5.26 \times 10^{8} \exp\left(-\frac{150{,}000}{RT}\right) \text{ cm}^2/\text{sec}$$

$$\delta_{Al} D^{b}_{Al} \text{ (2\% Fe)} = 8.48 \times 10^{-1} \exp\left(-\frac{105{,}000}{RT}\right) \text{ cm}^3/\text{sec}$$

This shift is due to an increase in cation lattice relative to anion grain boundary diffusion. Similar effects were found in polycrystalline Al_2O_3 doped with a mixed Mn - Ti impurity.

2.6 Creep of Polycrystalline Mullite

In last year's proposal preliminary data were presented on the steady state creep of fine-grained (5 - 6μm)* polycrystalline mullite at temperatures between 1350 and 1450°C. Polycrystalline billets of mullite were prepared by hot-pressing for 30-60 minutes at 1500°C and 6,000 psi. The powder was synthesized by a metal alkoxide process developed by Mazdiyasni and Brown [24]. The results of these experiments were published in a short note [1] which is attached to this report. Two significant results were reported: (1) the creep rate of polycrystalline mullite was nearly an order of magnitude lower than that of polycrystalline Al_2O_3 with a comparable grain size, (2) viscous creep was observed at 1400°C for stresses $\leq$ 400 kg/cm^2.

This year additional studies have been conducted to determine (1) the strain rate-stress dependence of higher temperatures, and (2) the effect of grain size on the steady state creep rate. Only a small range of grain sizes (1.5 - 5.0μm) were obtained. The microstructure of fine-grained mullite is evidently very stable, since annealing at temperatures up to 1700°C led to only a small amount of grain growth.

A summary of recent experiments at 1400 and 1450°C is presented in Table 12 for grain sizes in the range of 1.5 to 5μm. While viscous creep (N = 1) is dominant at 1400°C, non-viscous modes (N = 1.6 - 1.9) begin to appear at higher temperatures (1450°C). Secondly, the effect of grain size is much less than that expected from a diffusional creep mechanism. An increase in the grain size by a factor of ∿3 resulted in a decrease in creep

*linear intercept

Table 12

Effects of Grain Size on the Steady State Creep of Polycrystalline Mullite

σ = 100 kg/cm^2

Specimen	Strain Rate (h^{-1})	N*	Grain Size** (microns)	Temperature (°C)
A	1.60×10^{-4}	-	1.5	1450
B	1.30×10^{-4}	1.87	2.4	1450
C	1.42×10^{-4}	-	2.4	1450
D	0.96×10^{-4}	1.61	5.0	1450
E	3.40×10^{-5}	1.09	1.5	1400
F	3.30×10^{-5}	-	1.5	1400
G	2.65×10^{-5}	0.97	5.0	1400

*$\dot{\varepsilon} \alpha \sigma^N$; N = strain rate-stress exponent

**linear intercepts

rate by only a factor of 1.3 to 1.6 compared to factors of ∿9 and 27 expected for lattice and grain boundary diffusional creep processes, respectively. Further work is needed over a wider range of stresses and temperatures; however, it is clear from these preliminary results that the creep of polycrystalline mullite probably cannot be described by a simple diffusional mechanism.

III REFERENCES

1. P.A. Lessing, R.S. Gordon, and K.S. Mazdiyasni, "Creep of Polycrystalline Mullite" J. Amer. Ceram. Soc. 58 (3-4), 149 (1975).

2. Paul A. Lessing and Ronald S. Gordon, "Impurity and Grain Size Effects on the Creep of Polycrystalline Magnesia and Alumina" in Deformation of Ceramic Materials, Plenum Press, N.Y. Edited by R.C, Bradt and R.E. Tressler, pp 271-296, Plenum Press, N.Y. (1975).

3. R.S. Gordon, "Ambipolar Diffusion and its Application to Diffusion Creep", in Mass Transport Phenomena in Ceramics, edited by A.R. Cooper and A.H. Heuer, pp 445-464, Plenum Press, N.Y. (1975).

4. R.S. Gordon and J.D. Hodge, "Analysis of Mass Transport in the Diffusional Creep of Polycrystalline MgO-FeO-Fe_2O_3 Solid Solutions" Ronald S. Gordon and J. D. Hodge, J. Mater. Sci. 10 200-204 (1975).

5. G.R. Terwilliger, H.K. Bowen and R.S. Gordon, "Creep of Polycrystalline MgO and MgO-Fe_2O_3 Solid Solutions at High Temperatures," J. Amer. Ceram. Soc. 53 (5) 241-251 (1970).

6. R.S. Gordon, P.A. Lessing, and J.D. Hodge, "Impurity Effects on the Creep of Polycrystalline Magnesium and Aluminum Oxides at Elevated Temperatures," Technical Progress Report, AEC-COO-1591-27, December 1974.

7. R.S. Gordon, D.D. Marchant, and G.W. Hollenberg, "Effect of Small Amounts of Porosity on Grain Growth in Hot-Pressed Magnesium Oxide and Magnesiowüstite," J. Amer. Ceram. Soc. 53 (7) 1970.

8. R.T. Tremper, R.A. Giddings, J.D. Hodge, and R.S. Gordon, "Creep of Polycrystalline MgO-FeO-Fe_2O_3 Solid Solutions" J. Amer. Ceram. Soc. 57 (10) 421-428 (1974).

9. Ronald S. Gordon, "Mass Transport in the Diffusional Creep of Ionic Solids," J. Amer. Ceram. Soc., 56 (3) 147-152 (1973).

10. B.H. Hashimoto, M. Hama, and S. Shirasaki, "Preferential Diffusion of Oxygen Along Grain Boundaries in Polycrystalline MgO," J. Appl. Phys. 43 (11) 4828-29 (1972).

11. R.S. Gordon and G. R. Terwilliger, "Transient Creep in Fe-Doped Polycrystalline MgO" J. Amer. Ceram. Soc. 55 (9) 450-455 (1972).

12. W.C. Johnson, D.F. Stein, and R.W. Rice, "Analysis of Grain Boundary Impurities and Fluoride Additives in Hot-Pressed Oxides by Auger Electron Spectroscopy," J. Amer. Ceram. Soc. 57 (8) 1974.

13. J.M. Birch and B. Wilshire, "Work Hardening and Recovery During Compressive Creep of Polycrystalline MgO", J. Mater. Sci. 9 794-800 (1974).

14. J.B. Bilde-Sörensen, "Dislocation Structures in Creep-Deformed Polycrystalline MgO", J. Amer. Ceram. Soc. 55 606 (1972).

15. A.H. Heuer, R.M. Cannon, and N.J. Tighe, pp. 339-65 in Ultrafine-Grain Ceramics. Edited by J.J. Burke, N.L. Need, and Volker Weiss, Syracuse University Press, Syracuse, N.Y. (1970).

16. R.C. Folweiler, "Creep Behavior of Pore-Free Polycrystalline Aluminum Oxide," J. Appl. Phys., 32 773 (1961).

17. W.R. Cannon, "Mechanisms of High Temperature Creep in Polycrystalline Aluminum Oxide", Ph. D. Thesis, Stanford University, Stanford, CA, 1971.

18. Tadoaki Sugita and J.A. Pask, "Creep of Doped Polycrystalline Al_2O_3", J. Amer. Ceram. Soc. 53 609 (1970).

19. Glenn W. Hollenberg and Ronald S. Gordon, "Effect of Oxygen Partial Pressure on the Creep of Polycrystalline Al_2O_3 Doped with Cr, Fe or Ti," J. Amer. Ceram. Soc., 56 (3) 140-147 (1973).

20. R.M. Cannon and R. L. Coble "Review of Diffusional Creep of Al_2O_3," in Deformation of Ceramic Materials, edited by R.C. Bradt and R.E. Tressler, pp. 61 - 100, Plenum Press, N.Y. (1975).

21. R.E. Mistler, "Grain Boundary Diffusion Widths and Migration Kinetics in Aluminum Oxide, Sodium Chloride, and Silver". Sc.D. Thesis, Massachusetts Institute of Technology, Cambridge, Mass. (1967).

22. M.F. Ashby, "A First Report on Deformation Mechanism Maps", Acta. Met. 20 887-896 (1972).

23. T.G. Langdon, "Grain Boundary Deformation Processes" in Deformation of Ceramic Materials, edited by R.C. Bradt and R.E. Tressler, pp. 101-126, Plenum Press, N.Y. (1975).

24. K.S. Mazdiyasni and L.M. Brown, "Synthesis and Mechanical Properties of Stoichiometric Aluminum Silicate (Mullite)," J. Amer. Ceram. Soc., 55 548-52 (1972).

IV. BIBLIOGRAPHY OF PAPERS, THESES AND INVITED PRESENTATIONS

Papers

1. G.R. Terwilliger and Ronald S. Gordon, "Correlations Between Models for Time-Dependent Creep with Concurrent Grain Growth," J. Amer. Ceram. Soc. 54 (4) 218-219 (1969).

2. G.R. Terwilliger, H.K. Bowen, and Ronald S. Gordon, "Creep of Polycrystalline MgO-Fe_2O_3 Solid Solutions at High Temperatures," J. Amer. Ceram. Soc. 53 (5) 241-251 (1970).

3. Ronald S. Gordon, D.D. Marchant, and G.H. Hollenberg, "Effect of Small Amounts of Porosity on Grain Growth in Hot Pressed Magnesium Oxide and Magnesiowüstite," J. Amer. Ceram. Soc. 53 (7), 339-406 (1970).

4. G.W. Hollenberg, G.R. Terwilliger, and Ronald S. Gordon, "Calculations of Stresses and Strains in Four Point Bending Creep Tests," J. Amer. Ceram. Soc. 54 (4), 196-199 (1971).

5. D.D. Marchant and Ronald S. Gordon, "Grain Size Distributions and Grain Growth in MgO and MgO-Fe_2O_3 Solid Solutions," J. Amer. Ceram. Soc. 55 (1) 19-24 (1972).

6. Ronald S. Gordon and G.R. Terwilliger, "Transient Creep in Iron-Doped Polycrystalline MgO," J. Amer. Ceram. Soc. 55 (9) 450-455 (1972).

7. Glenn W. Hollenberg and Ronald S. Gordon, "Effect of Oxygen Partial Pressure on the Creep of Polycrystalline Al_2O_3 Doped with Cr, Fe, or Ti," J. Amer. Ceram. Soc. 56 (3) 140-147 (1973).

8. Ronald S. Gordon, "Mass Transport in the Diffusional Creep of Ionic Solids," J. Amer. Ceram. Soc. 56 (3)147-152 (1973).

9. G.W. Hollenberg and Ronald S. Gordon, "Origin of Anomalously High Activation Energies in the Sintering and Creep of Impure Refractory Oxides," J. Amer. Ceram. Soc, 56 (2) 109-110 (1973).

10. R.T. Tremper, R.A. Giddings, J.D. Hodge and Ronald S. Gordon, Creep of Polycrystalline MgO-FeO-Fe_2O_3 Solid Solutions," J. Amer. Ceram. Soc. 57 (10) 421-428 (1974).

11. Ronald S. Gordon and J.D. Hodge, "Analysis of Mass Transport in the Diffusional Creep of Polycrystalline MgO-FeO-Fe_2O_3 Solid Solutions," J. Mater. Sci. 10 200-204 (1975).

12. R.S. Gordon, "Ambipolar Diffusion and its Application to Diffusion Creep," in Mass Transport Phenomena in Ceramics, edited by A.R. Cooper and A.H. Heuer, pp 445-464, Plenum Press, N.Y. (1975).

13. P.A. Lessing and R.S. Gordon," Impurity and Grain Size Effects on the Creep of Polycrystalline Magnesia and Alumina" in Deformation of Ceramic Materials, edited by R.C. Bradt and R.E. Tressler, pp. 271-296, Plenun Press, N.Y. (1975).

14. P.A. Lessing, R.S. Gordon, and K.S. Mazdiyasni, "Creep of Polycrystalline Mullite," J. Amer. Ceram. Soc. 58 (3-4) 149 (1975).

13. P.A. Lessing and R.S. Gordon," Impurity and Grain Size Effects on the Creep of Polycrystalline Magnesia and Alumina" in Deformation of Ceramic Materials, edited by R.C. Bradt and R.E. Tressler, pp. 271-296, Plenun Press, N.Y. (1975).

14. P.A. Lessing, R.S. Gordon, and K.S. Mazdkiyasni, "Creep of Polycrystalline Mullite," J. Amer. Ceram. Soc. 58 (3-4) 149 (1975).

Theses

1. H.K. Bowen, "Creep of Magnesia," Senior Thesis, University of Utah (1967).

2. G.R. Terwilliger, "Creep of Polycrystalline Magnesia," Ph.D. Thesis, University of Uta (1968).

3. D.C. Moore, "Hot Pressing Magnesia with an Iron Dopant,"Senior Thesis, University of Utah (1970).

4. D.D. Marchant, "Grain Size Distributions and Grain Growth in MgO and MgO-Fe_2O_3 Solid Solutions," Senior Thesis, University of Utah (1968).

5. R.T. Tremper, "The Effect of Nonstoichiometry on the Creep of Iron-Doped Polycrystalline Magnesia," Ph.D. Thesis, Univeristy of Utah (1971).

6. G.W. Hollenberg, "The Effect of Oxygen Partial Pressure Changes on the Creep of Alumina Doped with Transition Metal Impurities (Cr, Ti, Fe)," Ph.D. Thesis, University of Utah (1972).

7. P.A. Lessing, "Thermogravimetric Analysis of Ti- and Fe-Doped Al_2O_3," Senior Thesis, University of Utah (1971).

8. P.A. Lessing, "Grain Size and Impurity Effects on the Creep of Polycrystalline MgO and Al_2O_3," Ph.D. Thesis, University of Utah (1975).

Invited Presentations

1. "The Effects of Impurities and Atmosphere on the Creep of Polycrystalline MgO," Materials Science Division, Argonne National Laboratory, April 1971.

2. "The Effects of Impurities and Atmosphere on the Creep of Polycyrstalline MgO and Al_2O_3," M.I.T., Lehigh University, Cornell University (1972).

3. "Mass Transport Processes in the High Temperature Creep of Polycrystalline Ceramics," Gordon Research Conference on Corrosion, July (1973).

4. "Impurity and Grain Size Effects on the Creep of Polycrystalline Magnesia and Alumina" Conference on Plastic Deformation of Ceramic Materials, Pennsylvania State University, July (1974).

5. "Ambipolar Diffusion and its Application to Diffusion Creep," University Conference on Ceramic Science, Case Western Reserve University, Cleveland, June (1974).

6. "Impurity and Grain Size Effects on the High Temperature Creep of Polycrystalline Al_2O_3 and MgO" Special Meeting Japanese Ceramic Society, Tokyo, Japan, June (1975).

V. ACKNOWLEDGEMENTS

The support of this research by the Energy Research and Development Administration under Contract No. E(11-1)-1591 is acknowledged.

VI. PRINCIPAL INVESTIGATOR

In addition to full time research on the contract for a portion of the summer, Dr. Gordon spends time throughout the year in supervisory activities and preparing talks and papers on work related to this contract.